Article

Frontal neurons driving competitive behaviour and ecology of social groups

S. William Li[1,2], Omer Zeliger[1,3], Leah Strahs[1,3], Raymundo Báez-Mendoza[1],
Lance M. Johnson[1,4], Aidan McDonald Wojciechowski[1,3] & Ziv M. Williams[1,5,6]✉

Competitive interactions have a vital role in the ecology of most animal species[1–3] and powerfully influence the behaviour of groups[4,5]. To succeed, individuals must exert effort based on not only the resources available but also the social rank and behaviour of other group members[2,6,7]. The single-cellular mechanisms that precisely drive competitive interactions or the behaviour of social groups, however, remain poorly understood. Here we developed a naturalistic group paradigm in which large cohorts of mice competitively foraged for food as we wirelessly tracked neuronal activities across thousands of unique interactions. By following the collective behaviour of the groups, we found neurons in the anterior cingulate that adaptively represented the social rank of the animals in relation to others. Although social rank was closely behaviourally linked to success, these cells disambiguated the relative rank of the mice from their competitive behaviour, and incorporated information about the resources available, the environment, and past success of the mice to influence their decisions. Using multiclass models, we show how these neurons tracked other individuals within the group and accurately predicted upcoming success. Using neuromodulation techniques, we also show how the neurons conditionally influenced competitive effort—increasing the effort of the animals only when they were more dominant to their groupmates and decreasing it when they were subordinate—effects that were not observed in other frontal lobe areas. Together, these findings reveal cingulate neurons that serve to adaptively drive competitive interactions and a putative process that could intermediate the social and economic behaviour of groups.

Competitive interactions have a profound influence on the behaviour of groups[1,2]. In most species, competitive success is closely linked to one's relative rank[3–5] and is characterized by the tendency of more dominant animals to monopolize food or forage more effectively than other group members[2,8,9]. It is also reflected by the ability of individuals to gauge their own social rank in relation to others and judge their environment in order to adjust competitive effort accordingly[2,6,7]. Previous animal studies using dyadic models of social behaviour have implicated areas such as the dorsomedial prefrontal cortex and anterior cingulate in establishing dominance hierarchies[3,10,11] and monitoring the behaviour of others[12–17]. They have also shown that these areas have a key role in establishing dominance relationships.

The cellular mechanisms that precisely drive the behaviour of groups or that link social rank with success, however, have remained less well understood. In particular, what has remained critically unclear is how one's relative rank within groups may be adaptively encoded by neurons or how such information influences foraging decisions when competing for food. Moreover, given that paired interactions are inherently linear (for example, pushing another in a tube test equals a higher

dominance)[10,11,15,18], it has not been possible to dissociate neural signals that reflect relative rank from those that specifically affect competitive behaviour, or to determine how competitive outcomes are influenced by one's own relative rank. It has also not been possible to determine how neural processes that influence competitive success precisely relate to those that drive reward-related decisions[19–22], or to determine how they affect the behaviour of groups ($n > 2$); especially under ethologically relevant conditions under which animals often interact[23]. Understanding the relationship between these social, economic and environmental factors that drive group behaviour has been a longstanding goal in ecology[2,6,7,9], but its cellular bases remain largely unknown.

Naturalistic group foraging paradigm

Mice often forage collectively within large social groups[24–26] and form stable dominance hierarchies that strongly influence the ability of individuals to successfully compete[27]. To study competitive interactions within social group settings and in a way that was amenable to single-neuronal analyses, we developed an ethologically based
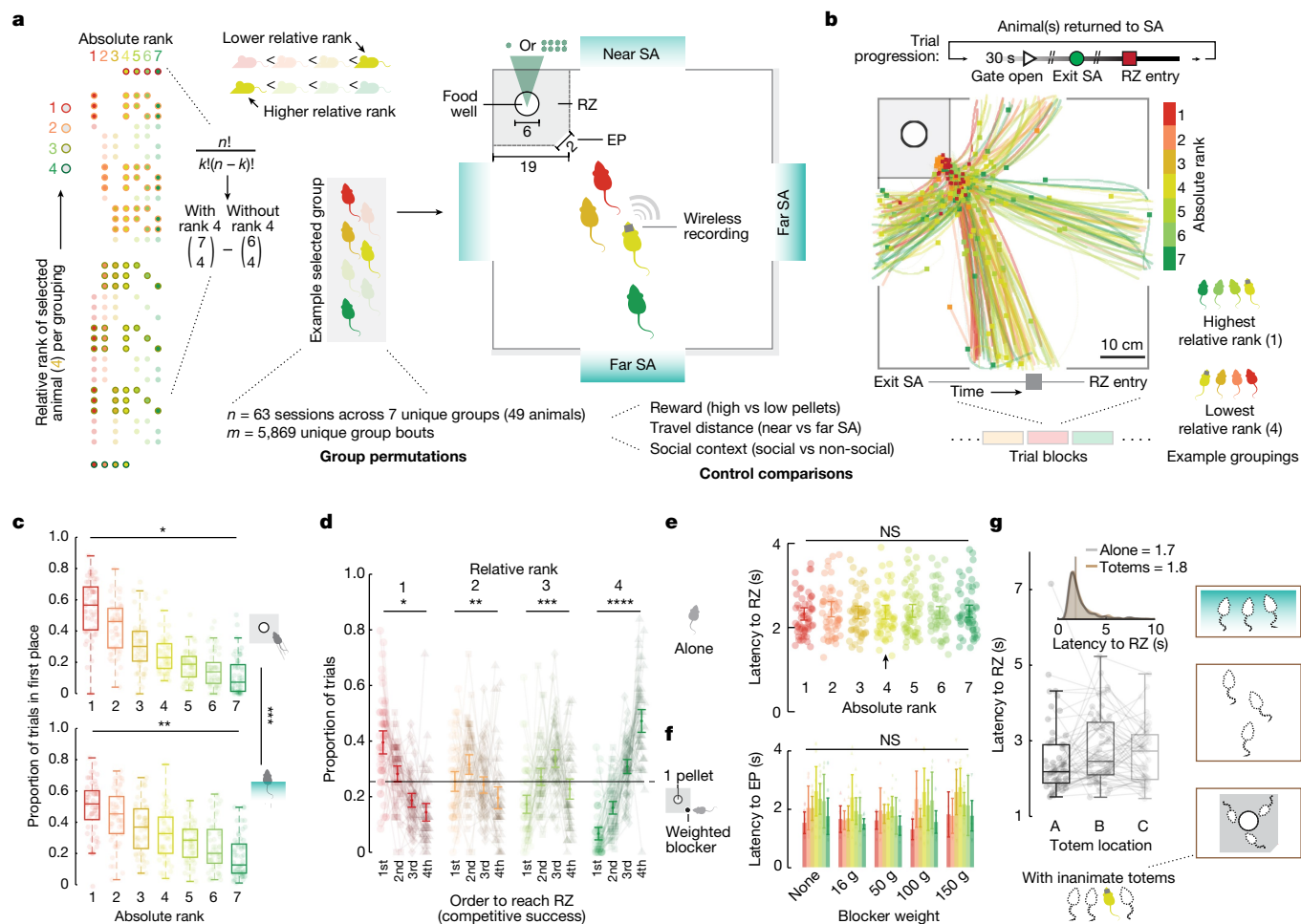
Fig. 1 | Naturalistic group foraging paradigm and competitive behaviour.
a, Competitive foraging paradigm and possible group permutations. Left, groups of four of seven possible mice foraged competitively in an arena across multiple groupings per session. An n-choose-k approach was used to vary the relative ranks of the mice. Right, within each session, the mice foraged under different economic (reward sizes), environmental (distance from staging area to reward zone) and social (relative rank or presence of social agents) conditions across blocks (Extended Data Fig. 1d, Supplementary Videos 1, 2). EP, entrance point; RZ, reward zone; SA, staging area. **b**, Real-time group competitive foraging. Top, trial and block design. Bottom, spatial trajectories of all mice across trials within a representative recording session. Squares indicate the instantaneous position of mice when the first mouse entered the reward zone (Extended Data Fig. 1e). **c**, Relationship between absolute dominance and success outcome (***$F_{(6,881)}$ = 2.71, P = 0.013; two-way ANOVA). The more dominant mice were more likely to be the first to reach the reward zone (top; *r_s = −0.69, P = 2.3 × 10^{-57}) and the first to exit the staging area (bottom; **r_s = −0.61, P = 2.3 × 10^{-41}). **d**, Relationship between relative rank and

competitive success. Mid-ranked mice were more likely to reach the reward zone earlier when higher in relative rank (*r_s = −0.72, P = 2.1 × 10^{-41}; **r_s = −0.15, P = 0.01) but less likely to reach the reward zone earlier when lower in relative rank (***r_s = 0.29, P = 3.8 × 10^{-6}; ****r_s = 0.86, P = 2.1 × 10^{-76}). **e**, Lack of difference in latency to reach the reward zone based on social rank when the mice foraged alone ($\chi^2_{(6,440)}$ = 6.79, P = 0.34; Kruskal-Wallis). Error bars in **d**, **e** denote mean ± 95% confidence interval (CI). **f**, Lack of difference in latency to reach the entrance point based on the weight of blockers that the mice were required to move to receive reward across social ranks (n = 26 mice; $F_{(24,255)}$ = 0.32, P = 0.99; two-way ANOVA). Error bars denote mean ± s.e.m. **g**, Lack of difference in latency to reach the entrance point when the mice foraged alone versus with inanimate totems (n = 7 mid-ranked mice; Z = 0.99, P = 0.32; signed-rank) as well as when the totems were placed in different locations (A, inside SA; B, outside SA; C, inside RZ) along the foraging path ($\chi^2_{(2,188)}$ = 4.24, P = 0.12; Kruskal-Wallis). For **c**–**e**, **g**, n = 63 sessions across 7 mice per rank (dots represent session averages). Box plot edges, 25th and 75th percentiles; centre line, median; whiskers, 1st–99th percentile range.

naturalistic group foraging paradigm in which nests of seven familiar male mice (n = 49 in total) freely competed for food (Fig. 1a, b, Extended Data Fig. 1a–e, Supplementaey Videos 1, 2). For each trial, in an arena, four of the seven mice competed to reach a reward zone containing food pellets and into which only one mouse could enter at a time, therefore establishing an explicit competitive order.

Next, to distinguish neural signals that may reflect the social rank of the mice from those that specifically reflect their success, we used an 'n-choose-k' approach ($n!/k!(n − k)!$) whereby four (k) of the seven (n) possible mice were randomly selected across groupings (Fig. 1a, Methods). To further distinguish neural signals reflecting the success of the animals from those representing the resources available or the

environments under which they had to compete, we also varied the amount of food reward (one versus eight pellets) and the travel distance (near versus far) over which the mice interacted (Extended Data Fig. 1d, Methods).

Finally, to track the collective behaviours of the mice, we used a custom-adapted video-tracking system that simultaneously recorded the position of each mouse (Methods). Miniaturized wireless multi-electrode microarrays were used to record single-neuronal activities and align them to trial events in real time at millisecond resolution. All trial conditions were controlled in a semi-automated fashion using customized electronics (Fig. 1b, Extended Data Fig. 1e). Together, we recorded 63 sessions for a total of 5,869 unique competitive bouts

(trials) interleaved in blocks of 7 bouts each. All mice maintained stable transitive dominance hierarchies over time (tube test[18]; $P > 0.2$; signed-rank; Extended Data Fig. 1b) and across dominance assays[24] (urine marking assay; Extended Data Fig. 1c). Neuronal recordings were always made from the mid-ranked mice.

Tracking group competition

Behaviourally, we found that the most dominant mice in their respective hierarchies were more likely to successfully compete for food[2,7,8] ($r_s = -0.69$, $P = 2.3 \times 10^{-57}$; Spearman correlation; Fig. 1c, Extended Data Fig. 1f–h). However, we also found that competitive success was highly dependent upon the animal's own relative rank compared to the other competitors (Fig. 1d, Extended Data Fig. 2). For example, the mid-ranked mice within each of their respective groupings were significantly more likely to succeed when competing with mice that were subordinate to them and significantly less likely to succeed when competing with those who were more dominant ($r_s = -0.72$, $P = 2.1 \times 10^{-41}$ and $r_s = 0.86$, $P = 2.1 \times 10^{-76}$, respectively; Spearman correlation). These behavioural effects were consistent when tested across animal groups and different ranks as well as between and within sessions (Extended Data Fig. 3). The effects were diminished, by contrast, when separating the mice before the start of the trial ($F_{divider*rank(6,223)} = 2.34$, $P = 0.032$; two-way ANOVA; Extended Data Fig. 4a–d), together suggesting that the mice adjusted their competitive behaviour on the basis of whom they specifically interacted with.

The more dominant animals were not simply faster or more fit. The mice showed no difference in the latency from gate opening to reach the reward zone based on absolute dominance when foraging alone ($\chi^2_{(6,440)} = 6.79$, $P = 0.34$; Kruskal-Wallis; Fig. 1e). They also showed no difference in the time taken to leave the staging area from gate opening ($\chi^2_{(6,440)} = 9.42$, $P = 0.15$; Kruskal-Wallis; Extended Data Fig. 2b). Similar findings were made when the mice were required to move a mass of variable weight at the entrance point to reach the reward zone ($F_{(24,255)} = 0.32$, $P = 0.99$; two-way ANOVA; Fig. 1f), as well as when foraging with inanimate totems positioned at different points in the arena ($Z = 0.99$, $P = 0.32$; signed-rank; Fig. 1g) or with totems that moved in a way that mimicked the naturalistic group foraging task (Extended Data Fig. 4e–k), further confirming that the behaviour of the mice indeed reflected their interaction with the other group members.

Finally, we evaluated the effect that the physical environment and amount of reward had on the animals' behaviour. Consistent with previous field observations[2,6,7], we found that higher amounts of reward and shorter minimum travel distance within the arena both led to shorter relative latency to reach reward ($F_{(1,1751)} = 9.13$, $P = 0.01$ and $F_{(1,1751)} = 24.9$, $P = 2.51 \times 10^{-5}$, respectively; three-way ANOVA; Extended Data Fig. 2a). Moreover, relative rank, reward size and distance had largely independent effects on the competitive outcomes of the mice ($P > 0.2$; three-way ANOVA). Together, these findings therefore suggested that the animals adjusted their competitive behaviour on the basis of the social (rank), economic (reward) and environmental (distance) conditions under which they had to compete.

Single-neuronal encoding of group behaviour

Neurons in the anterior cingulate encoded richly detailed information about the group behaviour of the mice. We stably recorded 1,049 well-isolated single units from the anterior cingulate cortex (ACC) across 7 unique groups (Fig. 2a, Extended Data Fig. 5a, Methods). First focusing on the animals' relative rank, competitive success and available amount of reward, we found that 53% ($n = 560$) of the recorded neurons exhibited task-related modulation ($P < 0.01$; false discovery rate (FDR) corrected for time epochs; three-way ANOVA; Methods). Of these neurons, 37% ($n = 208$) reflected the relative rank of the mice, meaning that they changed their activity according to whether other
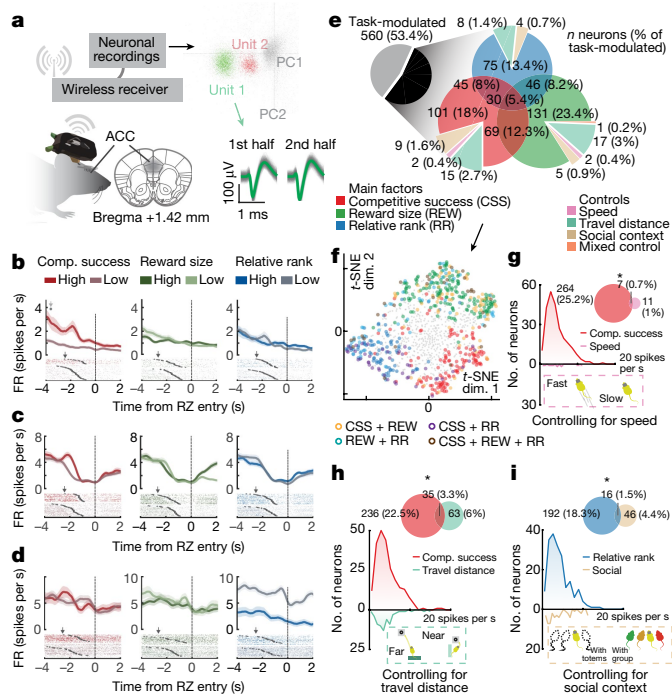

Fig. 2 | Single-neuronal representations of group behaviour. a, Left, illustration of the wireless micro-electrode and electrophysiological recording set-up (Extended Data Fig. 5a). Right, representative spike clusters and waveforms obtained from an electrode. PC, principal component. **b–d**, Peri-event histogram and spike raster plots of three representative neurons that showed changes in firing rate (FR) on the basis of the animals' competitive success (**b**), amount of reward (**c**) and relative rank (**d**). For all trials, neuronal activity is aligned to the time point at which the recorded mouse reached the reward zone. Grey dots represent the time of gate opening. Shaded areas denote mean ± s.e.m. (Extended Data Fig. 5b, c). **e**, Venn diagram illustrating the distribution of neurons that responded to differences in the mouse's relative rank (RR), reward size (REW) and/or competitive success (CSS; three-way ANOVA, $P < 0.01$; Extended Data Fig. 5d, e). **f**, t-distributed stochastic neighbour embedding (t-SNE) of the neural population's response patterns ($n = 1,049$ neurons). **g–i**, Venn diagrams illustrating the degree of overlap between neurons that responded to differences in the animals' competitive success and speed (**g**, $*\chi^2_{(1)} = 268$, $P = 3.3 \times 10^{-60}$; chi-square test), competitive success and distance needed to reach reward (**h**, $*\chi^2_{(1)} = 117$, $P = 3.3 \times 10^{-27}$; chi-square test) and relative rank and totem presence (**i**, $*\chi^2_{(1)} = 117$, $P = 3.3 \times 10^{-27}$; chi-square test). The distributions of neural activity are displayed, respectively, below.

group members were more dominant or subordinate to them. Other neurons (54%, $n = 301$), by comparison, reflected the amount of reward. Finally, 48% ($n = 271$) of the neurons reflected the competitive success of the mice, meaning that they showed a difference in activity based on whether the mice competed successfully. Most of the neurons that were modulated by the relative rank and success of the mice were found before gate opening or reaching reward entry, whereas most of the neurons modulated by reward were found after the mice entered the reward zone ($P < 0.05$; chi-square test; Fig. 2b–d, Extended Data Fig. 5b–d). These neurons therefore appeared to reflect the animals' group behaviour and competitive success (Fig. 2e, f).

Neurons that reflected the animals' competitive success were largely distinct from those that reflected their relative rank. Of the cells that responded to the relative rank of the mice, 8% responded to differences in success and, of all neurons, only 5% responded to relative rank, success and reward ($P < 0.001$; chi-square test; Fig. 2e, f, Extended Data Fig. 5e–g). Overall, most neurons showed little response to lower-level motoric factors such as the animal's speed (0.7%, $n = 7$) or physical proximity to others (0.9%, $n = 9$; Fig. 2g, h, Methods). Moreover, when
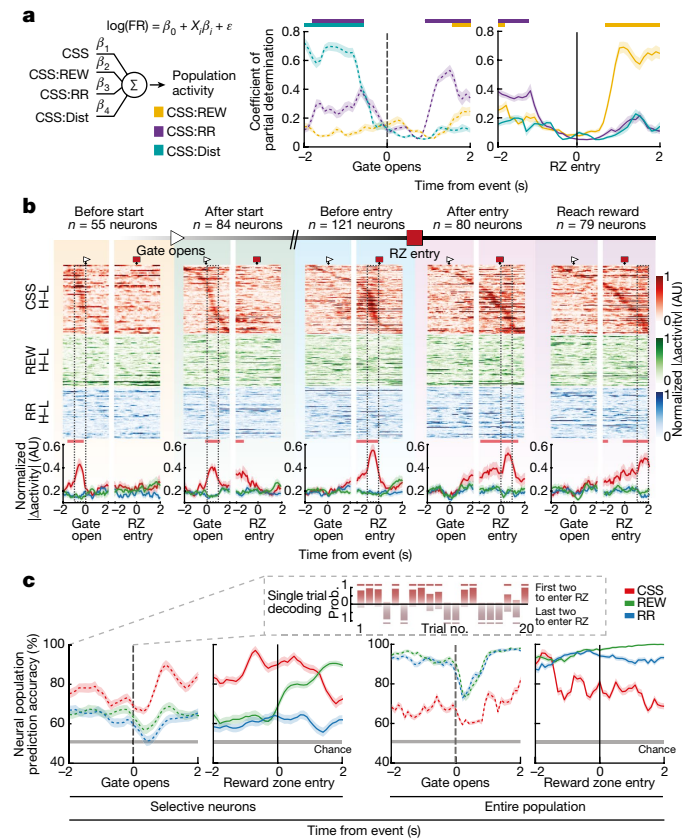
Fig. 3 | Modulation and neural population predictions of competitive success. a, Modulation of neural population response representing competitive outcomes. The fraction of explained variance (coefficient of partial determination) based on GLMs is provided for each task condition interaction with competitive success over the course of all trials. Horizontal bars depict time points in which the fraction of explained variance was higher than that expected from chance ($P < 0.01$; permutation test). Dist, travel distance. **b**, Temporal dynamic of neural population response. Top, heat maps of normalized activity for neurons that were modulated by the competitive success of the mice. H-L, high-low. AU, arbitrary units. Bottom, mean normalized change in activity for all neurons. Horizontal bars depict time points for which neural activity across conditions was significantly different ($P < 0.01$; one-way ANOVA). **c**, Support vector machines (SVMs) were used to quantify the degree to which competitive success could be predicted from neural population response. Inset, example of decoding projections using neural data on trials not used for model fitting ($n = 500$ bootstrapped samples). Projections reflect the predicted probability of upcoming competitive success on a trial-by-trial basis. Solid bars indicate correctly predicted trials; shaded bars indicate incorrectly predicted trials (Extended Data Fig. 8g–m). Shaded areas denote mean ± 95%CI.

replacing the other group members with inanimate totems, only 4.4% ($n = 46$) of the neurons reflected the animal's comparative 'success' based on the latency to reach the reward zone (Fig. 2i). These findings were largely consistent when tested across the different recorded mice (Extended Data Fig. 5h), sides of recordings[28] (Extended Data Fig. 5i), time (Extended Data Fig. 6a–f) and behavioural assays (Extended Data Fig. 6g–m). Therefore, although the upcoming success of the animals was closely behaviourally linked to their social rank, most single neurons that reflected the animals' relative rank showed little response in relation to their competitive behaviour.

Neuronal predictions of competitive success

Next, on the basis of these findings, we asked which neural processes precisely influenced the competitive behaviour of the mice. Using

generalized linear models (GLMs) that considered the effects that relative rank, reward amount and travel distance had on neural activities reflecting the animals' outcomes (Fig. 3a, Methods), we found that activities that reflect upcoming success were strongly modulated by the relative rank of the animals well before competition onset (Fig. 3a, b). Neural modulation by rank was significant before gate opening ($39.1 \pm 2.6\%$ peak variance explained; $P < 0.01$; permutation test), dropped at bout onset and then gradually increased until the mice reached the reward zone entry ($51.7 \pm 3.3\%$, $P < 0.01$; permutation test). Similar observations were also made in relation to the distance needed to reach the reward before gate opening ($68.5 \pm 3.1\%$, $P < 0.01$; permutation test), but not the overall amount of reward (Fig. 3a, b) or physical factors such as overtaking or pausing behaviour ($P > 0.05$; permutation test; Extended Data Fig. 7).

Collectively, the activities of these neurons were predictive of the upcoming success of the mice. Using multiclass models to decode competitive outcomes from neural data not used for model fitting (Methods), we found that the activities of the neurons were predictive of the animal's upcoming success before gate opening with an accuracy of $71.3 \pm 2.3\%$ ($P < 0.001$; permutation test; Fig. 3c, Extended Data Fig. 8a–e). Decoding accuracy then gradually increased over the course of competition, peaking at $94.3 \pm 2.6\%$ before reward zone entry ($P < 0.001$; permutation test). Decoding accuracies were otherwise near ceiling for relative rank and reward size throughout most of the trials (Fig. 3c). Overall, neural activities that reflected the upcoming success of the mice were influenced by prior trial outcomes well before competition onset ($47.8 \pm 5.5\%$ in the peak variance explained; $P < 0.001$; permutation test; Extended Data Fig. 8f–l). More notably, their activities predicted the upcoming success of the mice contingent upon their past reward outcomes with accuracy of up to $41.3 \pm 3.1\%$ ($H_0 = 25\%$, $P < 0.001$; permutation test; Extended Data Fig. 8i)—findings that were consistent over both short and long temporal scales (Extended Data Fig. 8j, k). Together, these neurons therefore appeared to integrate information not only about the animals' own relative rank but also about their past reward outcomes to influence their decisions.

Neural control of competitive effort

Finally, given these observations, we asked whether and how neural activity in the ACC causally affected the decisions of the mice animals. As noted above, a critical aspect of the group foraging paradigm is that it allowed us to dissociate the effects that neural activity had on the social rank of the animals from the effects that were specifically related to their competitive behaviour and success. Here, we used designer receptors exclusively activated by designer drugs (DREADDs) to focally excite or suppress cingulate activity (Fig. 4a, b, Extended Data Fig. 9a, b, Methods). Consistent with previous findings[10,11], we found that excitation of the ACC with clozapine-*N*-oxide (CNO) versus saline led to an increase in the animals' absolute dominance ranking in their respective hierarchies on tube testing ($Z = 2.61$, $P = 0.0046$; signed-rank; Fig. 4c, Extended Data Fig. 9c), whereas inhibition led to a decrease in the animals' absolute dominance ranking ($Z = -2.64$, $P = 0.0042$; signed-rank).

When tested during group foraging, however, we also found that the effect of neuromodulation on competitive behaviour was highly selective. Excitation of the ACC increased the competitive success of the mice when comparing CNO to saline, but only when the mice competed with others that were more dominant ($t_{(12)} = -2.6$, $P = 0.02$; paired *t*-test; Fig. 4d, e, Extended Data Fig. 9d). Inhibition, by contrast, decreased the animals' competitive success but only when competing with subordinates ($t_{(11)} = 2.14$, $P = 0.04$; paired *t*-test); these effects were highly consistent across rankings (excitatory: $t_{(12)} = -4.13$, $P = 0.0014$; inhibitory: $t_{(11)} = 3.05$, $P = 0.011$; paired *t*-tests) and 1.6 times larger than the variance in natural behaviour[14,22,29]. Therefore, rather than simply constitutively affecting competitive effort, neural activity in the ACC
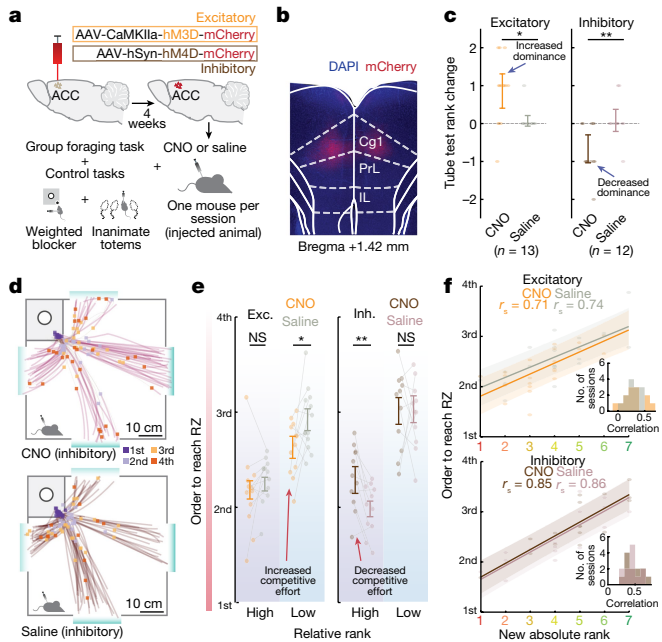
Fig. 4 | Selective control over competitive behaviour through ACC excitation and inhibition. a, DREADD-dependent excitation or inhibition of neural activity in the ACC (Extended Data Fig. 9a, b). **b**, DREADD expression in the ACC was confirmed histologically using mCherry fluorescence. cg1, cingulate area 1; IL, infralimbic cortex; PrL, prelimbic cortex. **c**, ACC excitation increased the social rank of the mice in their respective dominance hierarchies (n = 13 mice; *Z = −2.64, P = 0.0042; signed-rank) whereas inhibition decreased it (n = 12 mice; **Z = 2.61, P = 0.0046; signed-rank). **d**, Trajectories of the same mouse across foraging trials on two representative sessions (top, injected with CNO; bottom, injected with saline). Squares indicate the instantaneous position of the mouse when the first mouse in the group entered the reward zone, coloured by the order in which they entered. **e**, Left, competitive effort (based on order of reaching reward) was higher after CNO versus saline when the mice were ranked lower than their competitors (*$t_{(12)}$ = −2.6, P = 0.02) but not when they were ranked higher ($t_{(12)}$ = −0.12, P = 0.90). Right, competitive effort was lower after CNO versus saline when the mice were ranked higher than their competitors (**$t_{(11)}$ = 2.14, P = 0.038) but not when ranked lower ($t_{(11)}$ = −0.09, P = 0.93). **f**, Lack of relation between the other animals' competitive success and their rank within their respective dominance hierarchies for either excitation (n = 26 sessions; Z = 0.53, P = 0.59; signed-rank) or inhibition (n = 24 sessions; Z = 1.1, P = 0.27; signed-rank; Extended Data Fig. 9c–f). Error bars denote mean ± s.e.m. Dots represent session averages from each mouse.

conditionally influenced an animal's competitive effort on the basis of whom they specifically competed with.

Overall, neural modulation of the ACC had no effect on more generalized social behaviours such as aggression to suggest a nonspecific influence (Extended Data Fig. 9c). It also had no effect on behaviour when foraging alone (Extended Data Fig. 9e, f) and no effect on physical strength or speed (Extended Data Fig. 9g, h). Similarly, we found no selective effect on competitive behaviour when inhibiting the ventromedial prefrontal cortex (Extended Data Fig. 10) and no selective effect when inhibiting the nucleus accumbens, for which local inhibition led to a generalized loss of motivation and reward-seeking behaviour (Extended Data Fig. 10). The effect of neuromodulation in the ACC on the group behaviour of the animals was therefore both selective and specific.

Discussion

The behaviour of animals within groups is often driven by a complex interplay between diverse social, economic and environmental

factors[2,6,7,9]. It is also often affected by the individual's own social and physical attributes, which together can strongly influence their ability to successfully compete with other group members. The single-cellular mechanisms by which these factors influence competitive behaviour or affect the behaviour of individuals within social groups, however, have remained poorly understood. Here, using an ethologically based group foraging task together with wireless neuronal recordings and group tracking in mice, we found neurons in the ACC that not only encoded the animal's own social rank in relation to others but also reliably disambiguated their relative rank from their competitive behaviour. Together, these cells held detailed information about the social groups, the resources available and their local environment. Moreover, when modelled collectively, they reflected the relative rank and past rewards of the mice to reliably predict upcoming success—further suggesting that the neurons incorporated information about these ecological factors to influence the animals' decisions. Consistent with this hypothesis, neural excitation of the ACC increased the success of the mice but only when competing with more dominant groupmates, whereas inhibition decreased their success but only when competing with subordinates, together suggesting that the ACC had a specific and selective role in driving the competitive effort of the animals based on whom they interacted with. Determining how much effort to allocate when competing with others is essential to effective group living[8,30] and hinges on the ability of individuals to integrate information not only about the resources available but also about the social rank and behaviour of other group members to maximize benefit[2,6,7,9]. Our findings reveal a putative executive mechanism in the ACC, as part of the broader prefrontal cortical network, that could allow animals to evaluate social information about other group members and, based on this, provide a neural code that can adaptively influence competitive effort and outcome. They also suggest that competitive success is not simply a product of an animal's physical fitness or motoric ability but, rather, that it is strongly influenced by neural signals reflecting distinct social, economic and environmental factors that define their surroundings. Collectively, such signals would be essential for effective group behaviour and the ability of individuals to successfully compete.

Online content

Any methods, additional references, Nature Research reporting summaries, source data, extended data, supplementary information, acknowledgements, peer review information; details of author contributions and competing interests; and statements of data and code availability are available at https://doi.org/10.1038/s41586-021-04000-5.

1. Darwin, C. *On the Origin of Species by Means of Natural Selection, or, the Preservation of Favoured Races in the Struggle for Life* (John Murray, 1859).
2. Huntingford, F. A. & Turner, A. K. In *Animal Conflict* (eds Huntingford, F. A. & Turner, A. K.) 227–250 (Springer, 1987).
3. Zink, C. F. et al. Know your place: neural processing of social hierarchy in humans. *Neuron* **58**, 273–283 (2008).
4. Hoshaw, B. A., Evans, J. C., Mueller, B., Valentino, R. J. & Lucki, I. Social competition in rats: cell proliferation and behavior. *Behav. Brain Res.* **175**, 343–351 (2006).
5. Nagy, M., Akos, Z., Biro, D. & Vicsek, T. Hierarchical group dynamics in pigeon flocks. *Nature* **464**, 890–893 (2010).
6. Stephens, D. W. In *Encyclopedia of Ecology* (eds Jorgensen, S. E. & Fath, B.) 284–289 (Elsevier, 2008).
7. Clark, C. W. & Mangel, M. The evolutionary advantages of group foraging. *Theor. Popul. Biol.* **30**, 45–75 (1986).
8. Sapolsky, R. M. The influence of social hierarchy on primate health. *Science* **308**, 648–652 (2005).
9. Waite, T. A. The Bible of Social Foraging Theory. *Ecology* **82**, 906–907 (2001).
10. Zhou, T. et al. History of winning remodels thalamo-PFC circuit to reinforce social dominance. *Science* **357**, 162–168 (2017).
11. Wang, F. et al. Bidirectional control of social hierarchy by synaptic efficacy in medial prefrontal cortex. *Science* **334**, 693–697 (2011).
12. Levy, D. R. et al. Dynamics of social representation in the mouse prefrontal cortex. *Nat. Neurosci.* **22**, 2013–2022 (2019).
13. Allsop, S. A. et al. Corticoamygdala transfer of socially derived information gates observational learning. *Cell* **173**, 1329–1342 (2018).

Article

14. Haroush, K. & Williams, Z. M. Neuronal prediction of opponent's behavior during cooperative social interchange in primates. *Cell* **160**, 1233–1245 (2015).
15. Kingsbury, L. et al. Correlated neural activity and encoding of behavior across brains of socially interacting animals. *Cell* **178**, 429–446 (2019).
16. Lee, D. K. et al. Reduced sociability and social agency encoding in adult *Shank3*-mutant mice are restored through gene re-expression in real time. *Nat. Neurosci.* **24**, 1243–1255 (2021).
17. Dal Monte, O., Chu, C. C. J., Fagan, N. A. & Chang, S. W. C. Specialized medial prefrontal-amygdala coordination in other-regarding decision preference. *Nat. Neurosci.* **23**, 565–574 (2020).
18. Fan, Z. et al. Using the tube test to measure social hierarchy in mice. *Nat. Protoc.* **14**, 819–831 (2019).
19. Rushworth, M. F. & Behrens, T. E. Choice, uncertainty and value in prefrontal and cingulate cortex. *Nat. Neurosci.* **11**, 389–397 (2008).
20. Ruff, C. C. & Fehr, E. The neurobiology of rewards and values in social decision making. *Nat. Rev. Neurosci.* **15**, 549–562 (2014).
21. Cowen, S. L., Davis, G. A. & Nitz, D. A. Anterior cingulate neurons in the rat map anticipated effort and reward to their associated action sequences. *J. Neurophysiol.* **107**, 2393–2407 (2012).
22. Hillman, K. L. & Bilkey, D. K. Neural encoding of competitive effort in the anterior cingulate cortex. *Nat. Neurosci.* **15**, 1290–1297 (2012).
23. Pereira, T. D., Shaevitz, J. W. & Murthy, M. Quantifying behavior to understand the brain. *Nat. Neurosci.* **23**, 1537–1549 (2020).
24. Desjardins, C., Maruniak, J. A. & Bronson, F. H. Social rank in house mice: differentiation revealed by ultraviolet visualization of urinary marking patterns. *Science* **182**, 939–941 (1973).
25. Kareem, A. M. & Barnard, C. J. The importance of kinship and familiarity in social interactions between mice. *Anim. Behav.* **30**, 594–601 (1982).
26. Calhoun, J. B. The social aspects of population dynamics. *J. Mammal.* **33**, 139–159 (1952).
27. Williamson, C. M., Lee, W. & Curley, J. P. Temporal dynamics of social hierarchy formation and maintenance in male mice. *Anim. Behav.* **115**, 259–272 (2016).
28. Marlin, B. J., Mitre, M., D'Amour J, A., Chao, M. V. & Froemke, R. C. Oxytocin enables maternal behaviour by balancing cortical inhibition. *Nature* **520**, 499–504 (2015).
29. Baez-Mendoza, R., Harris, C. J. & Schultz, W. Activity of striatal neurons reflects social action and own reward. *Proc. Natl Acad. Sci. USA.* **110**, 16634–16639 (2013).
30. Snyder-Mackler, N. et al. Social determinants of health and survival in humans and other animals. *Science* **368**, eaax9553 (2020).

Methods

Animals

All procedures conformed to NIH Guidelines for the Care and Use of Laboratory Animals and were approved by the Massachusetts General Hospital IACUC. All experiments were performed on wild-type C57BL/6J male mice ($n = 98$) aged 2 to 5 months. Animals were bred from a lineage of mice received from Jackson Laboratories (stock no.000664). For all experiments, age- and weight-matched naive mice were randomly allocated in groups of seven animals to prevent potential behavioural confounds arising from kin[25,31] ($n = 7$ groups for neuronal recordings, $n = 2$ groups for inhibitory DREADDs, $n = 2$ groups for excitatory DRE-ADDs, $n = 2$ groups for reversible inactivation studies, $n = 3$ groups for divider control studies). Each experimental group was familiarized with each other by placing group members together in large (20 cm × 40 cm × 20 cm) cages and allowing them to freely interact for at least a week before experimentation. Abnormally aggressive mice (animals who caused injury to others) were removed and replaced with another animal until the group habituated to one another. Mice were maintained on a 12-h light–dark cycle (6 am to 6 pm) and were provided with food and water ad libitum outside of behavioural testing periods for foraging tasks specified below. For all foraging tasks, animals were kept at 85% of baseline body weight and had free access to water. All experiments were performed in the light phase of the 12-h cycle, which has been shown to reliably produce robust results as testing during the dark cycle[32].

Histology

For all histological experiments, animals were perfused transcardially with phosphate buffered saline (PBS) followed by 4% periodate-lysine-paraformaldehyde (PLP). Brains were extracted and post-fixed in 4% PLP for 48 h, washed 3 times in PBS, placed in 30% sucrose in PBS for 48 h and then sectioned at 50-mm thickness using a vibratome (Leica VT1200S). Slices were mounted with DAPI (Vectashield) and imaged with a fluorescence microscope. Images were combined and processed using ImageJ 1.52 (NIH).

Competitive group foraging task

Open-field apparatus and automated controls. To allow for open-field group interactions, the foraging task was performed in a 60 × 60 × 30 cm (W × L × H) open arena with a white acrylic floor bordered by opaque white acrylic walls. A 23 × 10 × 30 cm (W × L × H) walled 'staging area' adjoined the outer face of the arena on each side, centred on the arena face (Extended Data Fig. 1a, Supplementary Video 1). To control for environmental factors such as the travel distance and location from which the animals competed to reach the reward, the staging areas included two adjacent 'far' staging areas and two opposite 'near' staging areas. Here, custom-built automated, motorized and opaque guillotine gates permitted entrance into the arena from these staging areas at the beginning of each trial. To further control for the amount of food reward and its receipt by the animals, a 19 × 19 cm area in one corner of the arena was designated as the 'reward zone' and was partitioned from the rest of the arena by clear acrylic walls (Fig. 1a, Extended Data Fig. 1a). A white plastic cylindrical food well (6 × 1 cm D × H) was placed in the middle of the reward zone. A 14-mg pellet dispenser (ENV-203-14P, Med Associates) was affixed outside the arena and dispensed a user-specified number of 14-mg pellets (Dustless Precision Pellets, Bio-Serv) before the start of every trial relayed via a mini-IO box (Noldus). Plastic tubing (inner diameter: 0.7 cm) was fed from the dispenser (height: 22 cm) into the food well, such that dispensed reward pellets consistently landed in the food well and produced an audible sound that indicated to the animals how much food was available. Finally, to establish an explicit competitive order during the group competitions, a rectangular opening was cut (2 × 3.5 cm, W × H) at the bottom vertex of the 19 × 19-cm area, thus forming the 'reward zone entry' point. The height and width of the entrance were sufficient to permit

only one mouse to pass through at a time. All events were time-stamped and aligned with neuronal activity using a multi-unit acquisition system (MAP, Plexon) and microcontroller (Arduino Uno). For all experiments, the floor and walls of the arena and staging areas were cleaned with 70% ethanol followed by 1% acetic acid solution between groups and trial blocks. All experiments were conducted in a quiet room equipped with a white-noise sound machine (Marpac Dohm-DS).

Real-time simultaneous animal tracking. To track the individual mice, the fur of each mouse was bleached with a hair lightener and then stained with one of seven randomly assigned different semi-permanent natural dyes. For this, the mice were anaesthetized with isoflurane (5% for induction, 1.5–2.0% maintenance), and the fur was lightly bleached for 5 min over two consecutive days to prevent fur loss and then stained with a dye for 30 min. The dying process was repeated approximately every two weeks to maintain colour. Real-time, online spatial locations for each mouse were recorded using a colour-sensitive camera (Basler, acA1300-30gc) mounted 140 cm above the arena floor, at 30 fps. An EthoVision XT (Noldus) system was used to identify individual mice by their fur colour and record the 2D positions of each animal's nose-point (head), body and tail-base (tail) in real-time. Any missing data points were linearly interpolated by averaging the position immediately before and after (only 2.8% of all data was interpolated). Tracking data were smoothed using a locally estimated scatterplot smoothing (LOESS) method and any errors in detecting nose and tail were subsequently corrected using custom-written scripts in MATLAB (MathWorks). Finally, for validation, 1,000 random frames were manually scored for head, body and tail positions by two independent experimenters to evaluate the spatial and temporal precision of the tracking system, which gave an accuracy of 98.4% (with 1 cm degree of error).

Habituation and individual training. Before behavioural training, the mice were habituated in the open-field arena for 10 min over at least 3 separate days. After displaying decreased anxiety in the open field (more than 1 min spent in the centre), the mice were trained individually to pursue a food reward at the reward zone (Fig. 1a). Here, for each training trial, each mouse was placed in one of four staging areas. After 30 s, the gate for the staging area containing the animal opened, allowing it to freely forage for pellets that were dispensed into the food well before each trial. Trials ended 5 s after the mice entered the reward zone. Mice underwent at least 20 successive training trials per day, commencing at least five times from each of the four staging areas. Staging area locations and training order were randomized each day. Groups of seven were trained individually to forage for food pellets until criterion, defined by mean latency to reach the reward zone in less than 4 s and by a mean path error to the reward zone of less than 40°. The mice were also required to show no significant difference in these metrics for two consecutive days ($P > 0.05$; Kruskal-Wallis). On average, the mice underwent $14.7 ± 2.3$ training days ($294 ± 46$ total trials per animal) until criterion (mean ± s.e.m.), indicating that they were well habituated to the open-field arena. All mice used in the main experiments showed a stable transitive dominance hierarchy (Extended Data Fig. 1b).

Main task design and group permutations. Mice were placed inside the designated staging area at least 30 s before the start of the trial to prevent behavioural influence from experimenter handling. Either one pellet (low-reward condition) or eight pellets (high-reward condition) were dispensed into the food well 10 s before trial start. The dispensers provided the mice with an auditory cue before the trial start (1 click versus 8 clicks) indicating whether a small or large amount of reward was available in the reward zone. The automated gate opened once all four mice faced the gate simultaneously to ensure that variations in outcome were not due to simple spatial factors such as physical differences in position within the staging area. Trials ended 15 s after at least one mouse reached the reward zone, allowing animals to consume all

food pellets. Each experimental session for the main group experiments included 16 blocks (7 trials per block) of 'group' trials consisting of distinct group-foraging trial conditions. These blocks, in turn, introduced variations in the animals' relative rank (1, 2, 3 or 4) × staging area (far or near) × reward size (8 pellets or 1 pellet) given in pseudo-random order. An additional six non-social control blocks (four trials per block) in which the animals foraged alone with inanimate totems placed in one of three locations within the arena were also interleaved with the main blocks in pseudo-random order (Extended Data Fig. 1d).

Together, we used seven groups each consisting of seven mice. For each new session and day, four unique subgroups of four competitors (chosen from seven possible mice) were pseudo-randomly selected to participate in the session. To determine these subgroups, 4 mice were semi-randomly selected by $\binom{7}{4}$ so that the mid-rank (recorded) animal was always included in each subgroup and so that their competitors ran the same number of trials per session (Fig. 1a). Unique subgroups were tested once per trial condition (Extended Data Fig. 1d) and underwent four blocks of seven competition trials. Trial blocks were pseudo-randomized such that subgroups did not compete in consecutive blocks and were interspersed with 'totem' trials. Mice were returned to the large home cage at the end of each block and allowed a 5-min break period. Group members not performing the task ($n = 3$ for 'group' trials and $n = 6$ for 'totem' trials) remained in the large home cage. To control for the amount of food received per mouse over the course of a session, mice not participating in a given block were fed a number of pellets roughly equal to the average number of pellets consumed by participating mice. The first trial of each experimental block was excluded from analyses to avoid condition-switching effects. Therefore, when taken together, this combined approach allowed us to richly vary the relative rank, amount of reward, distance travelled and social context of the recorded animals' interaction with the other group members as we tracked their behaviour and neuronal activity at high spatial-and-temporal resolution.

Task controls

Control for fitness and motoric ability. Before every experimental day, each individual from a group of seven performed the foraging task alone for two blocks (one starting in a far and one starting in a near staging area; five trials) to confirm fitness (total: $n = 14$ randomly assigned blocks). If any animal differed significantly in task performance (latency to reach the reward zone; $P > 0.05$; Kruskal-Wallis) when running alone, we did not proceed with the full experiment.

Stationary non-social context control. To determine whether and to what degree the social context of the animals' interactions influenced their behaviour, we introduced an additional set of non-social controls. Here, each experimental session included six blocks of four trials each consisting of 'totem trials' in which we balanced distinct individual foraging trial conditions (staging area location (far or near) × totem location (inside staging area, outside, or inside reward zone); Fig. 1g, Extended Data Fig. 1d). Three life-like imitation mouse totems (Fun World) were placed either in the staging area (inside SA), in the arena outside of the reward zone (outside), or inside the reward zone (inside RZ) to mimic some of the possible locations the recorded mouse may physically encounter the other group members. Here, one food pellet was dispensed into the food well before each trial. The six totem trial blocks were pseudo-randomly interspersed with group competition blocks, such that no totem blocks were run consecutively.

Dynamic non-social context control. To further mimic the movements of other mice during the non-social context control, we repeated the stationary non-social context control but now had the totems actively move towards the reward zone. Here, the mice began each trial inside one of the two far staging areas along with three inanimate totems that were tied to a transparent fishing line (Berkley) and pulled towards the entrance point by an automatic retractable reel weighted to adjust the speed (Extended Data Fig. 4e). After the door opening, the totems travelled approximately 40 cm from the staging area to the entrance point of the reward zone while the animals 'competed' with the moving totems. During stationary trials, the totems and line were placed outside the reward zone as in 'outside' totem trials. Mice were returned to the home cage for 5 min between blocks. Within a given session, trials were divided evenly between two conditions (moving and stationary totems), as animals ran five trials starting from each staging area on the same day per condition ($n = 20$ trials per session). Two sessions were excluded in which mice were tripped by the fishing line.

Control for perseverance and strength. To evaluate differences in perseverance and strength of the animals, we developed a modified version of the group foraging task in which a weighted cylinder (16 g, 50 g, 100 g or 150 g) blocked the entrance point to the reward zone (Fig. 1h, Extended Data Fig. 4i–k). Here, the mice performed an abridged version of the group foraging task in which they individually foraged for one food pellet. Perseverance was determined by the latency for animals to reach the entrance point (weighted blocker), and strength was determined by the latency to push the blocker away and reach the reward zone. Experiments were performed in randomized blocks of six trials per staging area and per weighted cylinder. Blocks were pseudo-randomized in a linear round robin design.

Pre-trial partitioning control. To evaluate the effect that relative rank had on competitive success, the mice performed an additional control in which the identities of the group members were hidden from one another ('hidden') or revealed ('open') while in the staging area. During hidden trials, opaque non-perforated dividers partitioned the staging area into four 5.5 × 10 cm (W × L) compartments A, B, C, and D, where A is nearest to the entrance point and D is farthest (Extended Data Fig. 4a). Open trials followed the procedures as described above. For each experimental session, animals were pseudo-randomly divided into seven unique groups of four such that each mouse participated in an equal number of trials. Each experimental session comprised 28 blocks (4 trials per block), in which each group ran one combination of conditions (staging area (near or far) × identity knowledge (hidden or open)). Before each trial, four pellets were delivered into the food well in all trials. Within hidden blocks, the location of the mice within the partitioned staging area was further pseudo-randomized such that each mouse started in each partition exactly once to control for any effects of starting position on competitive performance. Before each hidden trial, mice were removed from their home cage and placed in their compartment sequentially to prevent interaction with their competitors. Therefore, even though all mice started their competitive bouts within the same staging area, they had no direct contact and no clear way of determining with whom they were competing until after gate opening.

Control for generalized aggression behaviour. To examine for differences in nonspecific social behaviour such as aggression, the mice were allowed to individually explore their home cage freely for 10 min (habituation). Feeding and water apparatuses were removed before habituation to allow unimpeded social interactions. After habituation, one novel age- and weight-matched adult wild-type C57BL/6 male mouse (intruder) was introduced into the cage and allowed to interact freely for 10 min. Intruder mice were group-housed and used for only one single encounter per day per subject mouse. Each experimental mouse underwent four such interactions separated by at least 24 h. Interactions were recorded using a ceiling-mounted digital camera (Canon Vixia, HF R500). All social interactive behaviours were scored manually by two blinded experimenters. Social inspection was defined by sniffing, direct contact or close following (less than 1 cm). Attack behaviour was defined as aggressive interactions such as chasing, attacking and wrestling or fighting. Defensive behaviour was defined as avoiding, fleeing and freezing.

Testing social dominance hierarchy

Tube test assay. Social dominance rank was determined using a modified version of the Lindzey Tube Test as described previously[18,33]. Two clear fibreglass tubes (30 × 3 cm; L × ID) were separated by an opaque acrylic divider that was operated manually (Extended Data Fig. 1b). The diameter of the tube was sufficiently wide to permit a mature mouse to pass through readily, but not sufficient to allow two mice to pass one another. Before testing began, each mouse was habituated to the tube apparatus for at least 10 min over 2 days to ensure that they would freely enter and exit the tube. During testing, pairs of mice were simultaneously placed into the ends of each tube with the middle divider in place. Mice entered the tube voluntarily. When both mice reached the middle of the apparatus, the divider was removed so that the mice directly faced one another. The manual opening of the divider triggered infrared sensors that activated video recording and real-time tracking with EthoVision XT (as above). Trials ended when one mouse forced the other to retreat out of the tube. To control against inherent side bias, trials were counterbalanced for a given pair in each subsequent repetition. Animal were declared the 'winner' when one mouse in the pair successfully forced a complete retreat from the other mouse in four consecutive trials. For each group of seven mice, a pseudo-random round robin design was carried out such that every possible dyad was tested within one day and no animal competed in consecutive pairings ($n = 21$ pairs per group). Hierarchical rank was determined by the collective outcomes of each pairing. Tube tests were repeated at the start of each experimental week ($n = 6$ total weeks; Extended Data Fig. 1b).

Urine marking assay. To verify group hierarchies, we used a modified version of the urine marking assay as described previously[24]. Here, each pair ($n = 21$ pairs per group) was placed in opposing sides of a two-chamber arena (30 × 30 × 30 cm, W × L × H) separated by a wire mesh partition (Extended Data Fig. 1c). Filter papers were placed below the arenas to absorb urine. Mice remained in the arenas for 4 h to allow for enough urine to collect and were then returned to their home cages for at least 30 min. Trials in which minimal urine was collected from either animal were repeated (7.6% of all pairings). Urine was fixed by 1% ninhydrin spray (N1411, Sigma), allowed to dry for 24 h and imaged with a camera. Urine markings were scored blindly using a custom GUI written in MATLAB. Each image was then manually cropped for both sides of the arena and centre partition was designated. Images were filtered for purple colour and converted to grayscale, and the intensity was manually adjusted to remove any background noise. The ratio of animal urine marks was calculated based on the number of pixels containing urine within 7 cm of the partition. All pairs were tested across 7 days (3 pairs per day) using a randomized round robin design.

Two-chamber assay. To confirm the consistency of relative rank encoding by neurons across behavioural assays, we used a modified two-chamber apparatus in which individual mice were paired together following the group competitive foraging assay within the same day. Here, we took advantage of our ability to continuously wirelessly record across assays to probe whether the representation of rank seen in the main foraging task can be replicated using a different social interaction assay for the same single neurons. We controlled for physical contact by using a two-chamber assay similar to those used in previous studies[34,35]. Approximately 20 min following the main group competitive forage recording session, pairs of mice within the group of seven were placed in opposing sides of a two-chamber arena (15 × 30 × 30 cm, W × L × H) separated by a wire mesh partition (Extended Data Fig. 6g). Mice freely explored the arena for three minutes while undergoing electrophysiological recordings, then were allowed to rest in their home cage for three minutes after each trial. A maximum of seven pairings (trials) were performed per session, with six animal pairings and one totem

pairing. Of the 63 group foraging sessions, we performed a total of 55 full two-chamber sessions and 3 partial sessions (owing to wireless head-stage battery constraints), resulting in a total of 305 unique social pairings. Bouts of the recorded mice investigating the cage mate or non-social totem were subsequently scored and verified manually by two blinded evaluators.

Testing for real-time behavioural kinematics

Behavioural kinematics. Behavioural variables that defined the performance of the mice during each trial included reaction time from gate opening, average path error, latency to the entrance point and latency to enter the reward zone. Reaction time to gate opening was calculated as the first time point at which any body part was visible in the arena. Path error was calculated by the difference in angle between the actual path of the mice and the optimal path to the reward zone entrance point while mice were in motion (velocity greater than 3 cm s^{-1}). Latency to the entrance point was calculated as the time from gate opening to the first time point when the nose-point of the mice was within 1 cm of the reward zone entrance from gate opening. Latency to the reward zone was calculated as the time from gate opening to the first time point when the entire body of the mice (all three body points) was inside the reward zone. The ratio of time occupying the reward zone was calculated by taking the cumulative amount of time that the mouse was inside the reward zone and then dividing each mouse's individual occupation time by the total time from all four mice.

In addition, we considered three ethological metrics that are often used to define competitive interactions[2,36,37] and which described the moment-by-moment physical dynamics of the mouse behaviours: overtaking, crowding and pausing. Overtaking events were defined as time points in which a mouse moved past another competitor (centre-point to centre-point distance < 5 cm) by taking the intersection of interpolated trajectories (distance over time) to the reward zone. If overtaking events occurred, the race positions were calculated based on the closeness of the mice to the reward zone in relation to the others. Crowding was defined as the number of competitors in proximity (centre-point to centre-point distance < 5 cm) to the recorded mouse outside the reward zone (less than 5 cm from the entrance point) and under conditions in which they were not markedly moving (velocity less than 3 cm s^{-1}). Pausing events were defined as time points when mice stopped or were not markedly moving (velocity less than 3 cm s^{-1}) for at least 200 ms after exiting the staging area.

Behavioural kinematic analysis. To determine how the moment-by-moment physical dynamics during foraging influenced the animal's outcomes, we examined how the pausing behaviour of the mice (t) was influenced by preceding overtaking events ($t − 1$; Extended Data Fig. 7). To this end, we constructed GLMs that took into simultaneous consideration (1) the animal's absolute rank; (2) the hierarchical rank difference between competitors; (3) the instantaneous velocity difference between competitors; (4) the proximity between competitors; (5) the instantaneous race position before the overtaking event; (6) the distance from reward at the time of the overtaking event. The GLM determined the effects of these covariates on the probability of pausing after an overtaking event:

$$\text{logit}(\text{pause}_t) = \beta_0 + \beta_1 \text{rank} + \beta_2 \text{rankdiff} + \beta_3 \text{velocitydiff}_{t-1}$$
$$+ \beta_4 \text{proximity}_{t-1} + \beta_5 \text{raceposition}_{t-1} + \beta_6 \text{distance}_{t-1}$$
$$+ \epsilon,$$

where pause$_t$ is the probability of a pausing event occurring at current time t (in seconds); β values are the regression coefficients for the different predictors; and ϵ is the residual term. The GLMs were used to evaluate the explanatory power of neuronal activity in relation to the animal's precise ordinal competitive order to reach the reward zone,

Article

relative rank and also the amount of reward available. We then tested significance for each regression coefficient using a standard *t*-test.

Finally, we examined whether and to what degree prior outcomes influenced competitive success in future trials (Extended Data Fig. 8l). For each trial *t* in which the mice competed, we categorized the trials as 'matching' or 'mismatching' depending on the outcome of the previous trial *t* − 1. We also categorized trial *t* as belonging within a persistent 'behavioural state' in which the competitive outcome was consistent over three or more trials (trials *t* − 1 and *t* − 2 must have had the same competitive outcome as trial *t*). A total of 47 of 63 sessions (701 out of the 1,049) were identified as containing enough trials (more than 3) in which animals were in persistent behavioural states.

Wireless single-neuronal recordings

Implantation of miniaturized multi-electrode arrays. Electrode implantations were performed on mid-ranked animals after habituation, foraging training and dominance hierarchy testing. Surgeries were performed under isoflurane anaesthesia (5% for induction, 1.5–2.0% maintenance). Floating microarrays consisting of 1–1.2-mm-long 500 kΩ platinum/iridium electrodes (Microprobes for the Life Sciences) were implanted in the ACC via 2.5 × 2.5-cm midline craniotomy centred at AP +1.2 mm from bregma. The array was lowered using a microdrive (David Kopf Instruments) and then secured with adhesive dental cement (Metabond, Parkell) followed by a dental acrylic (Jet) and jeweller's screws. Each array contained 16 microelectrodes (8 in each hemisphere) and 2 reference/ground electrodes located 1.2 mm below the cortical surface, targeting cg1/cg2 and the prelimbic cortex of the ACC. Neuronal recordings began at least two weeks after surgery to allow for recovery. After the completion of all recording experimentations, the location of microarray implantation was confirmed by electrolytic lesions (50 μa, 60 s, cathodal) and subsequent histology (below).

Wireless neuronal recordings. Neuronal signals were recorded via a detachable wireless head stage (Triangle Biosystems). The telemetry system consisted of a wireless transmitter connected to the microelectrode array through an Omnetics connector. A Plexon multichannel acquisition processor was used to amplify and band-pass-filter the neuronal signals (150 Hz–8 kHz; 1 pole low-cut and 3 pole high-cut with 1,000× gain; Plexon). Signals were then digitized at 40 kHz and processed to extract action potentials in real time by a Plexon MAP workstation. Putative single neurons were isolated from the recorded signal on the basis of their principal component analysis and waveform morphologies (Offline sorter, Plexon). Only single, well-isolated units (L ratio < 0.2 and isolation distance > 15) were used and all units were required to display a minimum threshold of 3 standard deviations above noise. All units were also required to demonstrate waveform morphology consistent with that of a cortical neuron (with a peak-to-trough 0.3 to 0.5 ms long) and to have at least 99% of spikes separated by a minimum refractory inter-spike interval of 2 ms. Any units that did not display stability (first two principal components) over the course of the recording session were excluded[38,39]. When an individual electrode recorded more than one putative neuron, a high degree of isolation was required to include each as a single unit (*P* < 0.01; multivariate ANOVA across the first two principal components). For each mouse, recordings were made across an average of 9 sessions (63 total) over the span of approximately 4 weeks. As done previously[12,13,40–44], we considered each single unit recorded across sessions as independent. Extended Data Figure 5h specifies the exact number of putative neurons recorded as well as active electrode channels per mouse. Firing rates and peri-event time histograms (PETHs) were calculated in 500-ms bins with a 100-ms sliding window, averaged across trials for each specific condition. No multi-units were used.

Neuronal analyses

Single-neuronal analysis. Neuronal firing activity was averaged over five 1-s task-relevant epochs: before gate opening, after gate opening,

before reward zone entry, after reward zone entry, and reaching reward (1–2 s after reward zone entry). First, a three-way analysis of variance (ANOVA, *P* < 0.01 with post-hoc comparisons; FDR corrected for multiple epochs) was performed on the main factors that described the animal's competitive interaction. These included the animal's relative rank (highest two versus lowest two in rank), reward size (one pellet versus eight pellets), travel distance (near versus far staging area), movement speed (fast versus slow), social context (foraging with groups versus foraging with totems) and competitive success (first two versus second two in order). Next, to account for the potential effects of prior trial outcomes (*t* − 1), we performed additional two-way ANOVAs (*P* < 0.01; FDR corrected for multiple epochs) on two main factors that included the current trial outcome (first two versus second two in order to reach the reward) and whether the previous trial outcome was matched or mismatched. Finally, to account for factors that described the physical interactions of the mice during competition, we included overtaking, crowding and pausing behaviours[3–5]. Here, activity was similarly analysed over 1-s epochs but now aligned to the events themselves (for example, activity ± 500 ms surrounding an overtaking event or activity ± 500 ms surrounding a 'crowding' event in which the mice were in close proximity). Here, comparisons were made across primary (rank, success, reward), secondary (travel distance, speed, context) and tertiary (proximity, overtaking, pausing) features that described the physical kinematics of the mice (three-way ANOVA, *P* < 0.01; FDR corrected for multiple epochs).

t-SNE. To visualize the organization of neuronal response within the population, we performed *t*-SNE procedure that transformed normalized activity for each main trial condition across each task-relevant epoch (3 × 5 dimensions) into a new 2-dimensional embedding space θ_{tsne}. This transformation used cosine distances between population tuning projections for three of the primary trial conditions (rank, success and reward). Each neuron was then labelled with its specific encoding properties for the three primary conditions (Fig. 2f) or epochs (Extended Data Fig. 5e).

Population modelling. Three separate GLMs were constructed to evaluate the population's response patterns. First, to examine neural responses to the precise ordinal competitive order and ordinal relative rank of the mice, we fitted a GLM to the activity of each neuron on the basis of the animal's ordinal order to reach the reward zone, reward size, and ordinal social rank relative to competitors:

$$\log(FR_n) = \beta_0 + \beta_1 oCSS + \beta_2 REW + \beta_3 oRR + \epsilon,$$

where FR_n is the firing rate of each *n* neuron; β values are the regression coefficients for the different predictors; and ϵ is the residual term. The GLMs were used to evaluate the explanatory power of neuronal activity in relation to the animal's precise ordinal competitive order to reach the reward zone (oCSS), relative rank (oRR), and the amount of reward available (REW). We tested significance for each regression coefficient using a standard *t*-test (*P* < 0.01; FDR corrected for multiple epochs).

Next, to further quantify the contribution (variance explained) of each trial variable that may be involved in the cost–benefit of neuronal encoding of competitive success during group foraging, we determined how the performance of the GLM declined when each variable was excluded from the model. Here, we defined the full model as:

$$\log(FR_p) = \beta_0 + \beta_1 CSS + \beta_2 CSS : REW + \beta_3 CSS : RR + \beta_4 CSS : Effort + \epsilon,$$

where FR_p is the firing rate of all neurons in the population; β values are the regression coefficients for the different predictors; ':' represents the interaction between each factor; and ϵ is the residual term. Here, as described previously[2,6,7,9], we specifically asked which factors might contribute to neural activity describing the animals' competitive

success. These predictors were defined by whole-trial variables as: CSS indicates competitive success; REW indicates reward size; RR indicates relative rank and Effort indicates staging area distance to reward zone.

Finally, to quantify the effect that past success or behavioural state (defined as three or more consecutive trials of the same competitive outcome; Extended Data Fig. 8f) had on neural activity reflecting the animal's current trial outcome, we quantified the degree to which GLM performance declined when each variable was excluded from the model. Here, we defined the full model as:

$$\log(\mathrm{FR}_p) = \beta_0 + \beta_1 \mathrm{CSS}_t + \beta_2 \mathrm{CSS}_t : \mathrm{CSS}_{t-1} + \beta_3 \mathrm{CSS}_t : \mathrm{State}_t + \epsilon,$$

where FR_p is the firing rate of all neurons in the population; β values are the regression coefficients for the different predictors; ':' represents the interaction between each factor; and ϵ is the residual term. These predictors were defined by whole-trial variables as: CSS indicates competitive success and State indicates presence of a persistent behavioural state at current trial t. Last, we evaluated the models with all predictors (full model) or individual predictors excluded (partial model). The coefficient of partial determination for each predictor was then calculated by comparing the variance explained of the partial model to the variance explained of the full model as defined by

$$\left(1 - \frac{R_{p,i}^2}{R_f^2}\right) \Big/ \sum_{k=1}^{4}\left(1 - \frac{R_{p,k}^2}{R_f^2}\right)$$

where $R_{p,i}^2$ is the variance explained of the partial model excluding the ith variable and R_f^2 is that of the full model. Partial models were refit such that new β values were generated with each excluded interaction variable. We resampled (bootstrap) the dataset 500 times to achieve contribution mean and error. To compare contributions of each trial variable, we performed one-way ANOVAs with Tukey's post-hoc tests across time.

Neural population predictions and decoding performance. SVMs were used to quantify the degree to which the upcoming success of the animals could be predicted from population response on a per-trial level[45,46]. These SVMs were constructed to find the optimal hyper-planes that best separate the data by performing:

$$\min_{w,b,\zeta}\left(\frac{1}{2}w^{\mathsf{T}}w + C\sum_{i=1}^{n}\zeta_i\right)$$

subject to:

$$y_i(w^{\mathsf{T}}\varphi(x_i) + b) \geq 1 - \zeta_i,$$

where $y \in \{1, -1\}^n$ corresponds to the one-versus-all classification for individual task features; x is the neural activity; and $\zeta_i = \max(0, 1 - y_i(wx_i - b))$. Here, we aggregated trial-by-trial firing rates of all recorded neurons and then divided the dataset into 80% for training and 20% for testing the model's predictions. To determine significance, this process was repeated 500 times and compared to models trained on neuronal data that were randomly shuffled (permutation test; $P < 0.001$).

Model-switch decoding. We examined the robustness of neuronal response to relative rank in two parts. First, during the two-chamber assay, we defined the times at which the mice investigated their partners by identifying time points at which subject mice engaged with the other animal. Then, we compared the firing rate of neurons at an epoch of 0–1 s after partner investigation when the recorded mice were paired with cage mates that were higher versus lower in rank relative to themselves ($P < 0.01$; Wilcoxon signed-rank). Next, to quantify the degree to which neural population responses to relative rank were consistent across the two social conditions, we used a model-switch approach in which we used SVM models (above) trained on neuronal activity during group foraging to decode the animal's relative rank from activity recorded during the two-chamber assay or vice versa.

Chemogenetic manipulation
Viral injections. AAV8-CaMKIIa-hM3D(Gq)-mCherry ($n = 13$ mice) and AAV8-hSyn-hM4D(Gi)-mCherry ($n = 12$ mice) were used for local excitation or inhibition of ACC neurons, respectively (Addgene). Isoflurane-anaesthetized mice were head-fixed on a Kopf stereotaxic frame, followed by bilateral craniotomies lateral of the sagittal suture and anterior of bregma. Using a syringe pump (Harvard Apparatus PHD Ultra) with 10-µl syringes (Hamilton 1700) and connected to 34 gauge needles (WPI NanoFil) by PE-10 and fused silica capillary tubing, we injected 200 nl of one of the virus constructs bilaterally (two injections per hemisphere, four total). We used the following coordinates relative to bregma: (1) AP +1.54 mm, DV −2.00 mm, ML ± 0.30 mm; (2) AP +0.98 mm, DV −2.00 mm, ML ± 0.30 mm. Mice were allowed to recover for 2–3 days before training and 4 weeks before CNO or saline injection experiments to allow for viral expression. Viral expression and anatomical location were confirmed by histology (Extended Data Fig. 9a, b). One mouse from the excitatory group and two mice from the inhibitory group were excluded owing to null viral expression.

Behavioural testing. Mice performed the same competitive foraging task and controls described above. Intraperitoneal (i.p.) injection of CNO (2–3 mg kg^{-1}; Tocris) or saline was given 30 min before the start of any behavioural testing, including the group foraging task, strength/perseverance assay, resident intruder assay and tube test. Mice also performed an abridged version of the tube task, in which the injected animal was paired against group mates in a round robin fashion. Animals were returned to the home cage and allowed to rest for at least 10 min before subsequent blocks of trials to avoid any effects from a history of winning or losing[10]. Resident intruder and perseverance assays were performed on separate days. Subsequent experiments were not performed for any injected animal or group of animals for at least 48 h after injection to allow for CNO washout. The same statistical analyses of behaviour were used as above.

Neurochemical manipulation
Neurochemical injections. As a separate control, the GABA$_A$ agonist muscimol was used to inhibit activity in the nucleus accumbens (NAc) or the ventral medial prefrontal cortex (vmPFC) within the same animals. Here, we implanted two pairs of 8-mm 23G stainless steel guide cannulas bilaterally to target the NAc and the vmPFC ($n = 6$ mice). The NAc cannulae were implanted at a 0° angle that extended to AP +1.18 mm, DV −3.3 mm, ML ± 1.00 mm from bregma. The vmPFC cannulae were implanted at a 10° angle that extended to AP +1.70 mm, DV −1.9 mm, ML ± 0.15 mm from bregma. Cannulae were secured using adhesive dental cement (Metabond, Parkell) and jeweller screws. Custom 8-mm 29G cannulae stylets were inserted into the cannulae at all times to prevent blockage. The mice were allowed two weeks of recovery after implantation before behavioural testing.

Behavioural testing. Mice performed the same competitive foraging task and controls described above. Before behavioural experiments, the animals were injected with either saline or muscimol (M1523, Millipore-Sigma) through either the NAc or the vmPFC cannulae in randomized fashion. Two 10-µl syringes (Hamilton), attached to an injection pump (Harvard Apparatus) were used to inject either 100 µl (NAc) or 200 µl (vmPFC) over 1 min through 9-mm 30G injection cannulae that extended 1 mm below the guide cannulae. The injection cannulae were left in place for an additional 5 min, and the mice were given a 30-min resting period before behavioural testing. For muscimol injections, we used a concentration of 0.2 mg ml^{-1} for the NAc to prevent motoric effects, and 1 mg ml^{-1} for the vmPFC. Cannulae placements were confirmed by histology after injection with a red fluorescent dye

Article

(Vybrant DiI, V22885, Invitrogen). The same statistical analyses of behaviour were used as above.

Statistics

Statical analyses were performed in MATLAB (MathWorks). Two-sided t-tests and ANOVAs were used on normally distributed data, whereas two-sided Wilcoxon rank-sum or signed-rank and Kruskal Wallis tests were performed on nonparametrically distributed data. Permutation tests were also used to avoid assumptions about the distributions of the data where appropriate. Regressions were analysed with Pearson's correlation if the data were continuous and Spearman's correlation if the data were ordinal. Significance of a regression was tested using the Wald t-test, and significance for the proportion of neurons were determined by chi-square tests. A P value of 0.05 was used as the threshold for a significant statistical difference unless noted otherwise. Data are expressed as mean ± s.e.m. unless noted otherwise. No statistical methods were used to predetermine sample size.

Reporting summary

Further information on research design is available in the Nature Research Reporting Summary linked to this paper.

Data availability

Additional behavioural and neuronal data that support the findings of the study are available from the corresponding author upon reasonable request. Source data are provided with this paper.

Code availability

All software packages used in this study are listed in the Reporting Summary along with their versions. The custom MALAB codes used to perform data and statistical analyses that support the findings of this study are available from the corresponding author upon reasonable request.

31. Manning, C. J., Wakeland, E. K. & Potts, W. K. Communal nesting patterns in mice implicate MHC genes in kin recognition. *Nature* **360**, 581–583 (1992).
32. Yang, M., Weber, M. D. & Crawley, J. N. Light phase testing of social behaviors: not a problem. *Front. Neurosci.* **2**, 186–191 (2008).
33. Lindzey, G., Winston, H. & Manosevitz, M. Social dominance in inbred mouse strains. *Nature* **191**, 474–476 (1961).
34. Xu, H. et al. A disinhibitory microcircuit mediates conditioned social fear in the prefrontal cortex. *Neuron*, **102**, 668–682 (2019).
35. Murugan, M. et al. Combined social and spatial coding in a descending projection from the prefrontal cortex. *Cell* **171**, 1663–1677 (2017).
36. Olsson, I. A. S. et al. Understanding behaviour: the relevance of ethological approaches in laboratory animal science. *Appl. Anim. Behav. Sci.* **81**, 245–264 (2003).
37. Dewsbury, D. A. Comparative psychology, ethology, and animal behavior. *Annu. Rev. Psychol.* **40**, 581–602 (1989).
38. Musallam, S., Bak, M. J., Troyk, P. R. & Andersen, R. A. A floating metal microelectrode array for chronic implantation. *J. Neurosci. Methods* **160**, 122–127 (2007).
39. Prasad, A. et al. Abiotic-biotic characterization of Pt/Ir microelectrode arrays in chronic implants. *Front. Neuroeng.* **7**, 2 (2014).
40. Gremel, C. M. & Costa, R. M. Orbitofrontal and striatal circuits dynamically encode the shift between goal-directed and habitual actions. *Nat. Commun.* **4**, 2264 (2013).
41. Han, W. et al. Integrated control of predatory hunting by the central nucleus of the amygdala. *Cell* **168**, 311–324 (2017).
42. Scheggia, D. et al. Somatostatin interneurons in the prefrontal cortex control affective state discrimination in mice. *Nat. Neurosci.* **23**, 47–60 (2020).
43. Gehrlach, D. A. et al. Aversive state processing in the posterior insular cortex. *Nat. Neurosci.* **22**, 1424–1437 (2019).
44. Klavir, O., Prigge, M., Sarel, A., Paz, R. & Yizhar, O. Manipulating fear associations via optogenetic modulation of amygdala inputs to prefrontal cortex. *Nat. Neurosci.* **20**, 836–844 (2017).
45. Hung, C. P., Kreiman, G., Poggio, T. & DiCarlo, J. J. Fast readout of object identity from macaque inferior temporal cortex. *Science* **310**, 863–866 (2005).
46. Wasserman, L. *All of Statistics: a Concise Course in Statistical Inference* (Springer Texts, 2004).

a Foraging apparatus

b Measuring social dominance hierarchy and confirming stability

c Confirming social dominance across assays

d Task conditions

e Example trials

Relation between reaction time and competitive success

f

g

h

Extended Data Fig. 1 | See next page for caption.

Article

Extended Data Fig. 1 | Group foraging task and dominance assays. a, A 3-D representation of the custom-designed arena with automated gates and food dispenser. Measurements are in cm. **b**, A tube test assay was used to evaluate the linear and transitive dominance hierarchies of the animals (n=7 unique groups totaling 49 animals over 6 weeks). The absolute ranks of the animals were confirmed to be stable over time (p>0.2 across all ranks and experimental weeks; Signed-rank). Error bars denote mean ± s.e.m. **c**, A urine marking assay was used to confirm the robustness of social dominance hierarchy across assays. The ratio of pixels with urine are displayed for each pairings of animals arranged based on their rank in the dominance hierarchies as determined by the tube test assay (mean ± s.e.m.; *n*=7 unique pairs across permutations). **d**, Schematic representation of the main task conditions and their permutation. The different primary economic (reward sizes), environmental (distance from staging area to reward zone) and social (relative rank or presence of social agents) conditions are displayed along the margins. Timeline of an example session where trials were run in a pseudo-randomized block design is shown in the middle. **e**, Example trials from one session depicting trajectories from all four possible staging areas (Fig. 1b). **f**, Heat maps showing increased latency (Left) and increased order (Right) to reach the reward zone with decreasing absolute hierarchical and relative ranks. Mean ± s.e.m. **g**, Heat maps showing increased time (Left) and increased order (Right) to exit the staging area with decreasing absolute hierarchical and relative ranks. Mean ± s.e.m. **h**, Spearman correlation between reaction time and competitive success. Heat map showing decreased correlation between reaction time (i.e. order to exit the staging area) and competitive success (i.e. order to reach the reward zone) with decreasing absolute hierarchical and relative ranks. For panels **f**–**h**, n=7 animals per absolute rank, across n=63 sessions. Dots represent session averages.

**a** Relation between rank, reward size and travel distance

Reaction time

Group rank variance
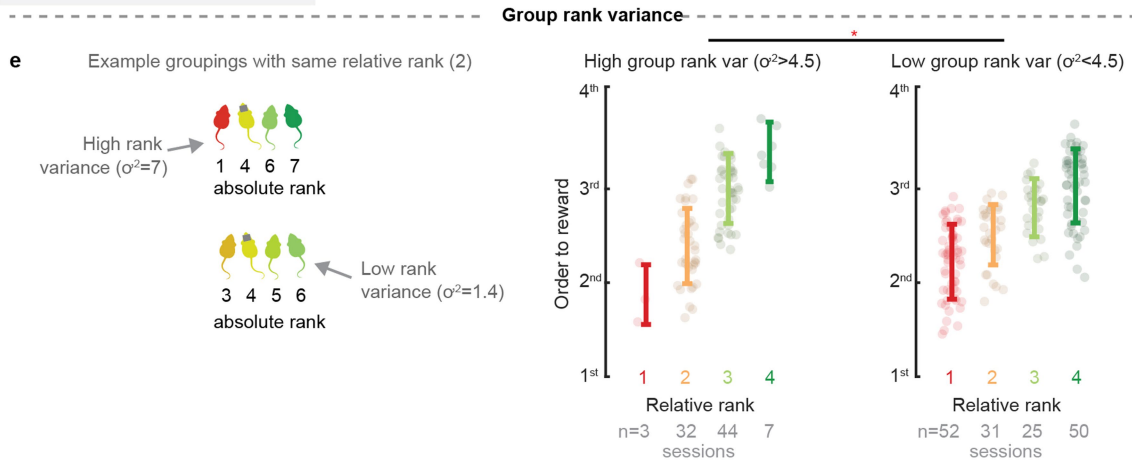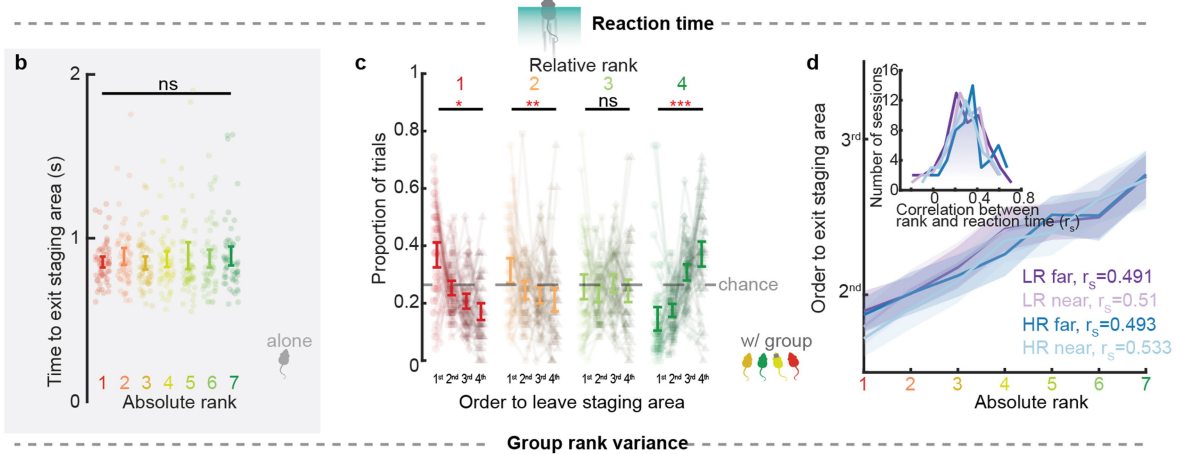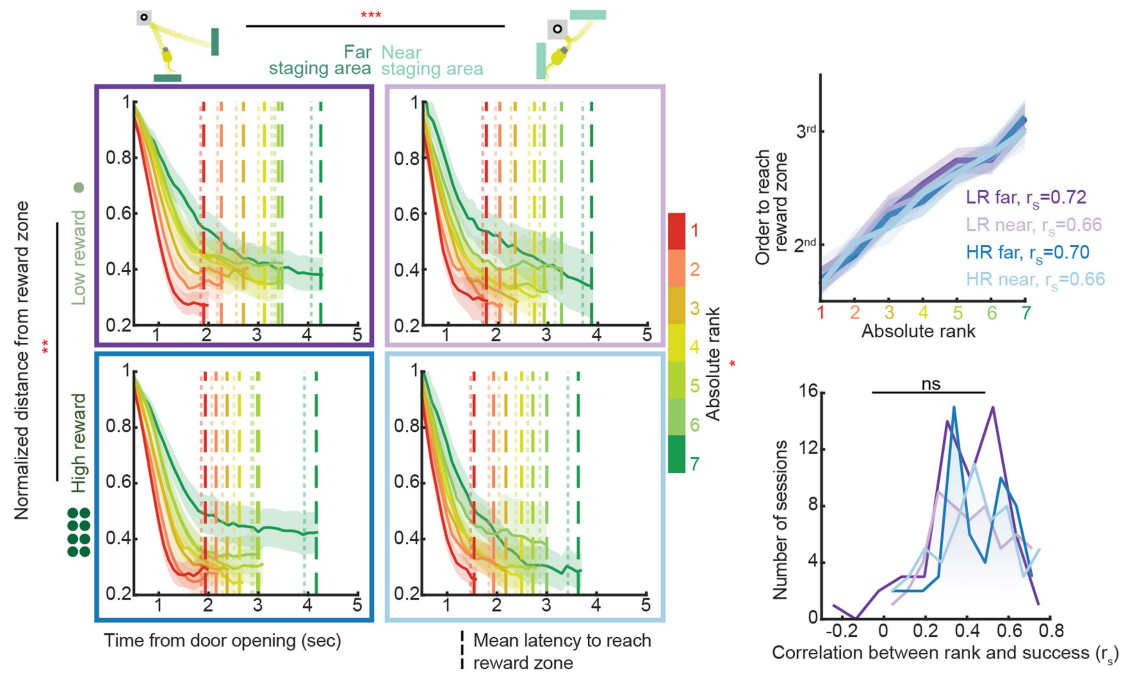
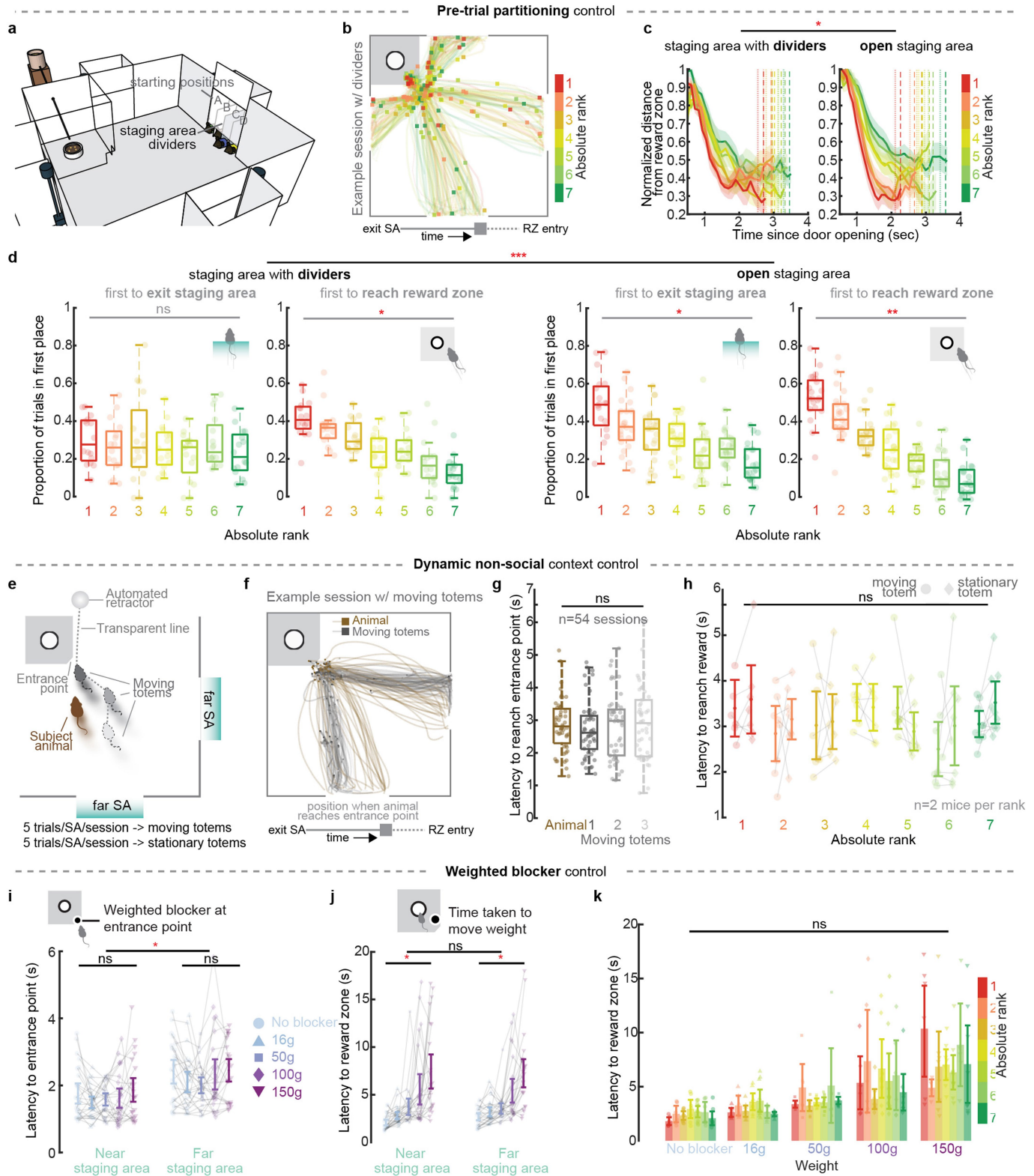**Extended Data Fig. 2** | See next page for caption.

Article

Extended Data Fig. 2 | Confirming the relation between relative rank and competitive success across different metrics. a, To evaluate the independent effect that reward amount or travel distance may have on the animals' behaviour, we varied both the staging area from which the animals started and amount of food. Left, The animals reached the reward zone faster on high reward trials (**$F_{(1,1751)}$=9.13, p=0.01) and on trials where they started from the near staging areas (***$F_{(1,1751)}$=24.9, p=2.51x10^{-5}). However, there was no interaction between terms describing the animals rank, reward amount or distance ($F_{rank:reward(6,1751)}$=0.25, p=0.96; $F_{rank:stagingarea(6,1751)}$=0.33, p=0.92; $F_{reward:stagingarea(1,1751)}$=2.58, p=0.11; $F_{rank:reward:stagingarea(6,1751)}$=0.4, p=0.88; three-way ANOVA). Right, Similar findings were also made when performing a within-session spearman correlation values across all trial conditions ($F_{(3,251)}$=0.51, p=0.67; one-way ANOVA). **b**, There was no significant difference in reaction time when animals ran the task alone on control trials prior to the start of group trials ($\chi^2_{(6,440)}$=9.42, p=0.15; Kruskal-Wallis). Error bars denote mean±95%CI. **c**, The mid-ranked animal was more likely to react faster (i.e. leaving the staging area faster than others) in the group competition task at lower relative ranks (1 and 2; *r_s=-0.55, p=1.4x10^{-21}, **r_s=-0.34, p=2.2x10^{-8}) and to react slower at higher relative rank (4; ***r_s=0.68, p=2.3x10^{-35}) but not at rank 3 (r_s=-0.04, p=0.5). Error bars denote mean±95%CI. **d**, Hierarchical rank within a group was correlated with reaction time across all trial conditions. Spearman correlation calculated across sessions (n=63). Inset, There was no difference in within-session spearman correlation values across all trial conditions ($F_{(3,251)}$=1.11, p=0.35; one-way ANOVA). Shaded areas denote mean±95%CI. **e**, Left, Graphical depiction of high vs low rank variance groupings. Right, Although relative rank was positively correlated with competitive success in both high and low rank variance trials, there was a significant interaction between group rank variance and the animals' relative rank in influencing the animals' competitive success (n=63 total sessions per high vs low rank variance; *$F_{rankvar:relrank(3,265)}$=3.94, p=0.009; two-way ANOVA). Together, these findings suggested that, even when controlling for the animals' rank relative to conspecific competitors, the specific rank of others played a significant role in adjusting the animal's competitive behaviour. Error bars denote mean ± s.e.m. For all panels, n=7 animals per absolute rank, across n=63 sessions. Dots represent session averages.
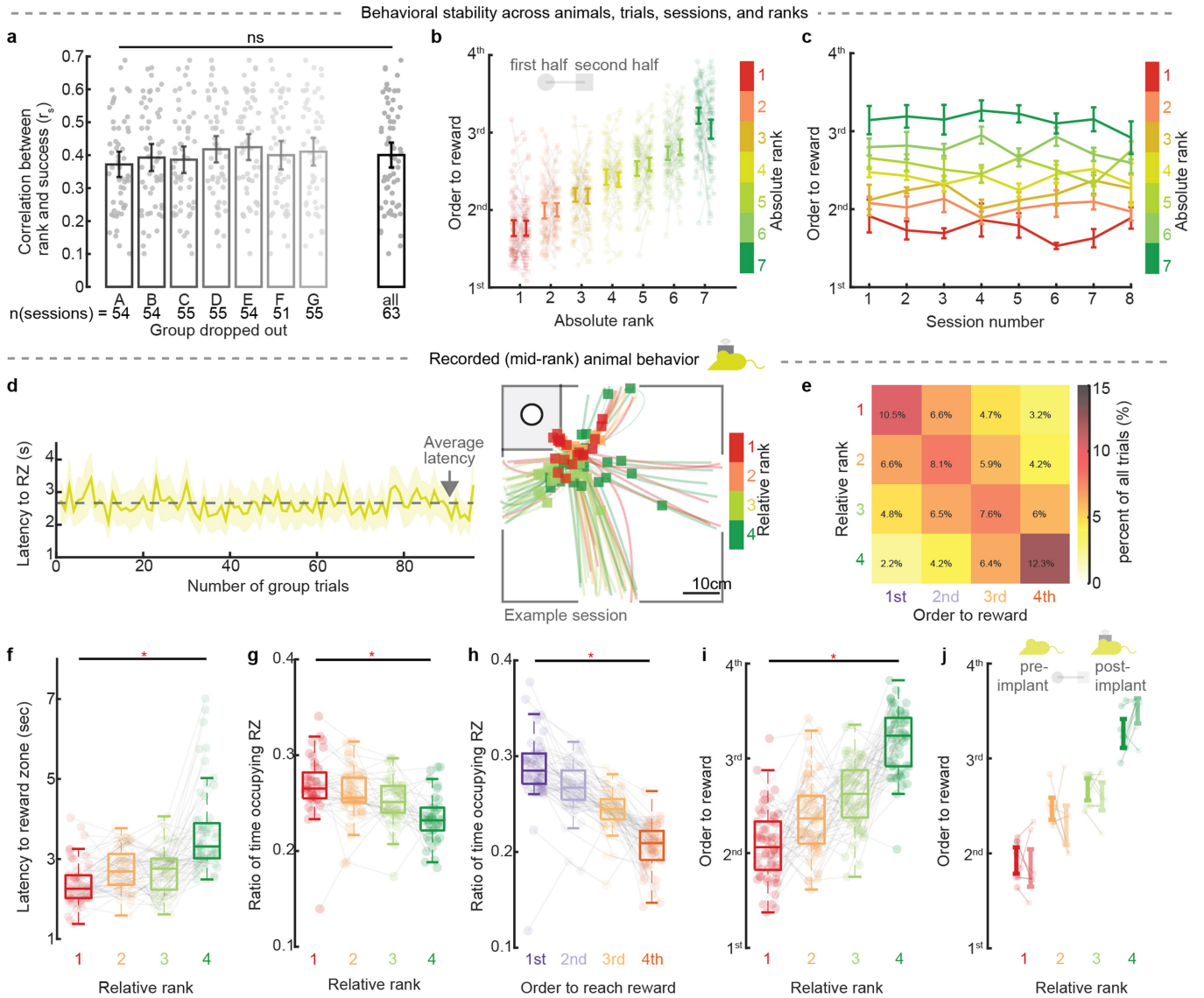
**Extended Data Fig. 3 | Relation between social rank and competitive
success. a**, Group-dropping procedure demonstrated a consistent behavioural
correlation between hierarchical rank and competitive success across all
groups ($F_{(7,440)}=0.68$, p=0.69; one-way ANOVA), suggesting that no particular
groups(s) disproportionately affected the main behavioural results. Error bars
denote mean±95%CI. **b**, There was no difference in the animals' competitive
success between the first and second half of each session ($F_{rank(6,872)}=0.025$,
p=0.70; two-way RM-ANOVA) and no interaction between terms that defined
the animal's rank and time period ($F_{rank*time(6,872)}=0.21$, p=0.27; two-way
RM-ANOVA); suggesting that the animals' overall competitive success was
stable within individual sessions. Error bars denote mean±95%CI. **c**, Comparing
the animals' original dominance rank to the order in which the same animals
reached reward during foraging demonstrated that competitive success did
not significantly differ over consecutive sessions (n=7 groups of 7 mice
per session; $F_{sessionNumber(7,391)}=0.21$, p=0.98; two-way RM-ANOVA). There was no
interaction between terms that defined the animal's rank and session number
($F_{sessionNumber*rank(42,391)}=0.103$, p=0.80; two-way RM-ANOVA). Error bars denote
mean ± s.e.m. **d**, Left, The mid-rank (recorded) animals' latency to the reward
zone was stable across the duration of the entire session (n=63 sessions; p>0.1
for all time points; one-sample *t*-test), indicating that motivation for food was
consistent throughout the session. Right, Representative behavioural
trajectories of the recorded animal across all group trials in one session (same
session as shown in Fig. 1b). There were no differences in motoric behaviour

between the recorded animal (the mid-ranked animal having the head stage)
compared to its groupmates. Squares indicate the instantaneous position of
the animal when the first animal in the group entered the reward zone (RZ),
coloured by the recorded animal's relative rank. **e**, Heat map showing the
percentage of trials where the relative ranking of animals exactly matched
their competitive success. The animals' relative ranks and the order in which
they reached reward matched exactly on 38.5% of the foraging trials and at a
proportion that was significantly higher than expected from chance
(p<0.05, Permutation tests; across all comparisons). **f**, Latency to reach the
reward zone was dependent on the animal's relative rankings when foraging in
groups (*r_s=0.8, p=3.1x10^{-58}). The mid-ranked animals spent more time
occupying the reward zone compared to competitors when they were more
dominant relative to others (**g**, *r_s=-0.46, p=1.78x10^{-10}; Spearman correlation)
as well as when they reached the reward zone prior to others (**h**, *r_s=-0.80,
p=2.46x10^{-51}; Spearman correlation). **i**, The animals' relative ranks and the
order in which they reached reward were significantly correlated on a
session-by-session basis (*r_s=0.77, p=2.17x10^{-47}; Spearman correlation).
j, Competitive success was stable following electrode implantation (n=4 animals,
n=2 sessions pre-implant and first 2 sessions post-implant; $F_{implant(1,63)}=0.16$,
p=0.69; one-way RM-ANOVA). Error bars denote mean ± s.e.m. For panels
b, **f**–**i**, dots represent session averages (n=63). Box-plot edges represent
25th/75th percentiles with center=median and whiskers=1st-99th percentile
range.

Article

Extended Data Fig. 4 | See next page for caption.

Extended Data Fig. 4 | Task controls and behavioural performances. a, A 3-D representation of the custom-designed arena with automated gates and food dispenser (Extended Data Fig. 1) but with dividers now placed in the staging area (SA) for the pre-trial partitioning control. **b**, Spatial trajectories of all animals across all trials within one representative session with SA dividers. Squares indicate the instantaneous position of the animals when the first mouse reaches the reward zone (RZ). **c**, Higher ranked animals displayed greater success when compared to their subordinates both in trials with and without SA partitioning (r_s=0.419, p=9.1x10^{-7} for divider trials; r_s=0.593, p=1.22x10^{-16} for open trials; Spearman correlation). The presence of dividers, however, significantly affected the effect that the animals' rank had on their competitive success (*$F_{divider*rank(6,223)}$=2.34, p=0.032; two-way ANOVA). N=16 sessions across n=3 unique groups of 7 mice. Shaded areas denote mean±95%CI. **d**, Left, For trials with SA partitioning, the dominant animals were more likely to be the first to reach the reward zone compared to subordinate partners (*r_s=-0.702, p=6.74x10^{-18}; Spearman correlation). However, there was no relation between dominance rank and leaving the staging area (r_s=-0.095, p=0.12). Right, In trials without SA partitioning, the dominant animals were more likely to be the first to exit the staging area (*r_s=-0.43, p=2.41x10^{-6}) and reach the reward zone (*r_s=-0.742, p=8.15x10^{-21}). There was a significant interaction between the animal's absolute dominance in their respective hierarchies and the presence of dividers in the staging area (***$F_{divider*rank(6,447)}$=2.58, p=0.018; two-way ANOVA), together suggesting that the animals took into account information about the relative ranks of the other animals both prior to and after trial start during competition. N=16 sessions across n=3 unique groups of 7 mice. **e**, Graphic depicting a dynamic non-social context control where inanimate totems were pulled from the staging area until the entrance point of the reward zone using an automated retractor while one mouse foraged for a food pellet (see Methods). **f**, Spatial trajectories of all moving totems and mouse across all trials within one representative session. Squares indicate the instantaneous position of the animals and totems when

the mouse reached the entrance point. **g**, The mice and moving totems reached the entrance point at approximately the same time (n=54 sessions across n=14 mice; $F_{(3,197)}$=0.27, p=0.85; one-way ANOVA). **h**, There were no main effects of hierarchical rank ($F_{rank(6,107)}$=0.89, p=0.50; two-way RM-ANOVA) or interaction effects of rank and totem movement ($F_{rank*totemtype(6,107)}$=0.68, p=0.67; two-way RM-ANOVA) on the animals' latency to reach reward during the totem trials; together suggesting that presence of the moving totems did not influence the animals' behaviour. There was no difference in latency to reach the reward zone based on absolute dominance rank when the animals foraged alone. N=54 total sessions across n=2 mice per rank. Error bars denote mean±95%CI. **i**, To evaluate whether the more dominant animals were stronger or were more perseverant, the animals were required to move a mass of variable weight at the reward entrance point. There was no significant difference in latency for animals to reach the entrance point between different weighted blockers ($F_{(4,255)}$=2.16, p=0.07) but did display an expected difference in for the different staging areas (*$F_{(1,255)}$=35.2, p≈0). There was no interaction between terms describing the weight amount and staging area location ($F_{(4,255)}$=0.23, p=0.92; Two-way ANOVA). N=26 mice per blocker weight. Error bars denote mean±95%CI. **j**, There was a significant difference in latency to enter the reward zone based on the weight of the blockers (*$F_{(4,255)}$=27.9, p≈0), but no difference between staging area locations ($F_{(1,255)}$=0.08, p=0.78). There was no interaction between terms describing the weight amount and staging area location ($F_{(4,255)}$=0.25, p=0.91; Two-way ANOVA). N=26 mice per blocker weight. Error bars denote mean±95%CI. **k**, There was no difference in latency to enter the reward zone based on ranks across any of the weights ($F_{(24,255)}$=7.9, p=0.32; Two-way ANOVA); suggesting that hierarchical rank did not significantly affect the animals' strength or perseverance. N=26 mice per blocker weight (n=3,3,4,4,5,3,4 for absolute ranks 1-7, respectively). Error bars denote mean ± s.e.m. Dots represent session averages. Box-plot edges represent 25th/75th percentiles with centre=median and whiskers=1st-99th percentile range.
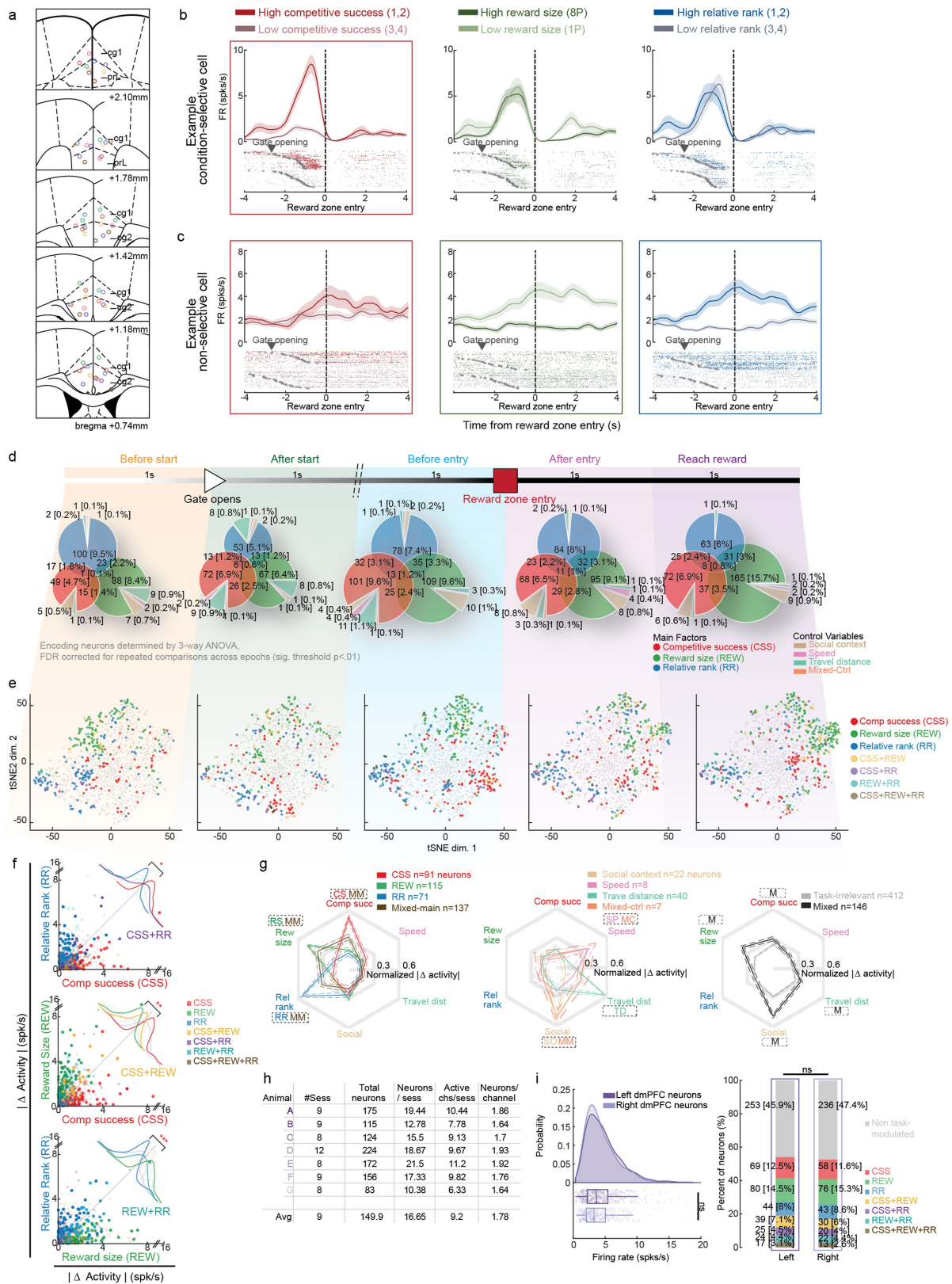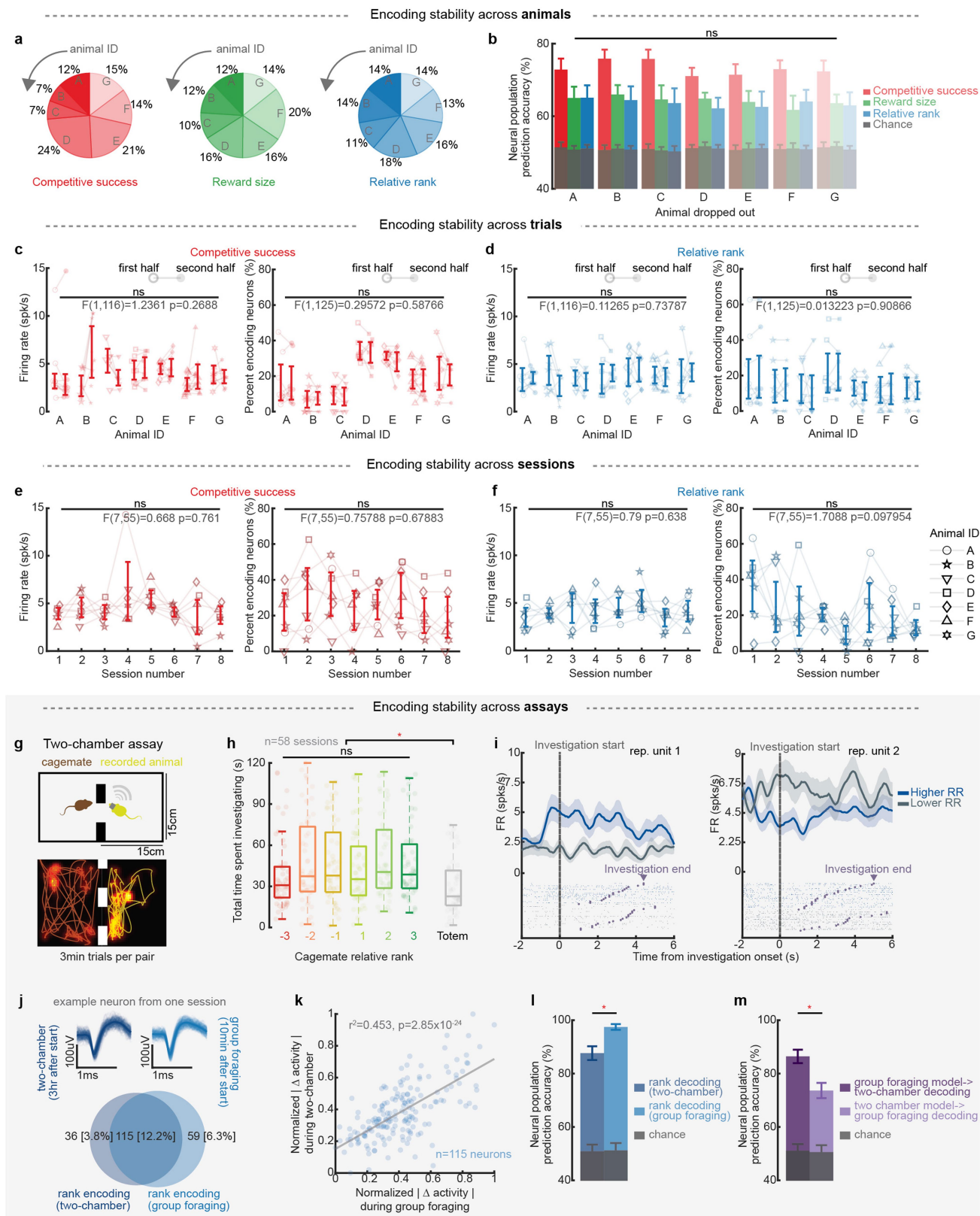
Extended Data Fig. 5 | See next page for caption.

Extended Data Fig. 5 | Temporal dynamic of neural population response.
a, Electrode localization for all recorded animals (n=7), colour-coded for each mouse. cg1/cg2=cingulate areas 1/2; prL=prelimbic cortex; iL=infralimbic cortex. **b**, Peri-event histogram (PETH) and spike rasters a neuron that displayed a selective change in firing rate for only high vs low competitive success trials. PETHs are aligned to when the recorded animal enters the reward zone. Grey dots represent gate opening (i.e. trial start). **c**, PETH and spike rasters of a neuron that did not display selective changes in firing rate change. PETHs are aligned to when the recorded animal enters the reward zone. Grey dots represent gate opening. **d**, Recruitment of ACC neurons over the course of the trials. For each epoch, each Venn diagram depicts the distribution of neurons within the recorded population that responded differentially to the three primary factors that described the animals' competitive interactions: competitive success (CSS), reward size (REW), and relative hierarchical rank (RR) across all task-relevant epochs. For each main factor, embedded pie charts show the proportion of overlapping cells based on their encoding properties. **e**, For each epoch, all recorded neurons are highlighted and labelled with colours corresponding to their specific encoding properties on the same t-SNE space as shown in Fig. 2f. Dots represent each recorded neuron (n=1049 from 7 mice). Grey dots represent neurons that displayed no task-related modulation. **f**, Scatter plots illustrating the absolute difference in neuronal activities *per* neuron across the three main task conditions. Here, dots represent each recorded neuron (n=1049 from 7 mice) and are colour-coded based on whether they each displayed significant differences in response to relative rank, reward and success. Primary comparisons were made between competitive success vs. reward (*Z=10.8, p=3.4x10^{-27}; Rank-sum), competitive success vs. relative rank (**Z=7.48, p=7.7x10^{-14}; Rank-sum) and relative rank vs. reward (***Z=10.29, p=8.14x10^{-25}; Rank-sum). **g**, Polar plots illustrating the relative tuning of neurons that responded to differences in the animal's relative rank, reward size and competitive success. For comparison, polar plots are also provided for neurons that responded to differences in speed (SP); travel distance (TD), social context (SO), mixture of controls (MC) and mixture of all task conditions (M). Polar plot for cells that responded to none of these task features is shown in grey. Dashed boxes represent significance limits for each condition (p<0.01; Kruskal-Wallis with one-sided Holm-Sidak correction for post hoc comparisons). The s.e.m. for each polar plot is given as dashed lines. **h**, Table displaying the average number of putative neurons and active electrode channels per recorded animal. **i**, Left, firing rates for neurons recorded from left and right hemispheres (t_{1047}=1.64, p=0.10; two-sided t-test). Right, there was no difference in the encoding proportions for any of the main features of the group competitive foraging task between neurons recorded from the left versus right hemispheres (p>0.05, Chi-square tests). Box-plot edges represent 25th/75th percentiles with centre=median and whiskers=1st-99th percentile range.

Article

Encoding stability across **trials**

Encoding stability across **sessions**

Encoding stability across **assays**

Extended Data Fig. 6 | See next page for caption.

Extended Data Fig. 6 | Stability of neuronal encoding across animals, sessions and assay. a, Normalized proportion of neuronal encoding competitive success, reward size, and relative rank across animals. **b**, An animal-dropping procedure revealed no difference in peak decoding performance for competitive success, reward size, and relative rank across animals ($F_{(6,1399)}=1.27$, $p=0.20$ for competitive success, $F_{(6,1399)}=0.89$, $p=0.69$ for reward size, and $F_{(6,1399)}=0.44$, $p=0.98$ for relative rank; one-way ANOVA). **c**, Population firing rates and proportion of neurons encoding competitive success were stable across trials within sessions (n=63 sessions across 7 animals; $F_{(1,116)}=1.24$, $p=0.27$ for firing rate; $F_{(1,125)}=0.30$, $p=0.59$ for proportion of encoding neurons; two-way RM-ANOVA). **d**, Population firing rates and proportion of neurons encoding relative rank were stable across trials within sessions (n=63 sessions across 7 animals; $F_{(1,116)}=0.11$, $p=0.74$ for firing rate; $F_{(1,125)}=0.013$, $p=0.909$ for proportion of encoding neurons; two-way RM-ANOVA). **e**, Population firing rates and proportion of neurons encoding competitive success were stable across sessions (n=63 sessions across 7 animals; $F_{(7,55)}=0.67$, $p=0.76$ for firing rate; $F_{(7,55)}=0.758$, $p=0.679$ for proportion of encoding neurons; two-way RM-ANOVA). **f**, Population firing rates and proportion of neurons encoding relative rank were stable across sessions (n=63 sessions across 7 animals; $F_{(7,55)}=0.79$, $p=0.64$ for firing rate; $F_{(7,55)}=1.709$, $p=0.098$ for proportion of encoding neurons; two-way RM-ANOVA). **g**, Top, Graphic showing the two-chamber arena in which the recorded animal was placed with cagemates following each group foraging session. Bottom, Heat map and trajectories of both animals during a representative trial. **h**, Animals spent similar amount of time investigating the other animal regardless of their hierarchical rank relative to the recorded animal ($\chi^2_{(5,304)}=5.63$, $p=0.34$; Kruskal-Wallis), but spent significantly less time investigating inanimate totems (Z=4.13, $p=3.64\times10^{-5}$; Rank-sum). Dots represent trials (n=376) across n=58 sessions. Box-plot edges represe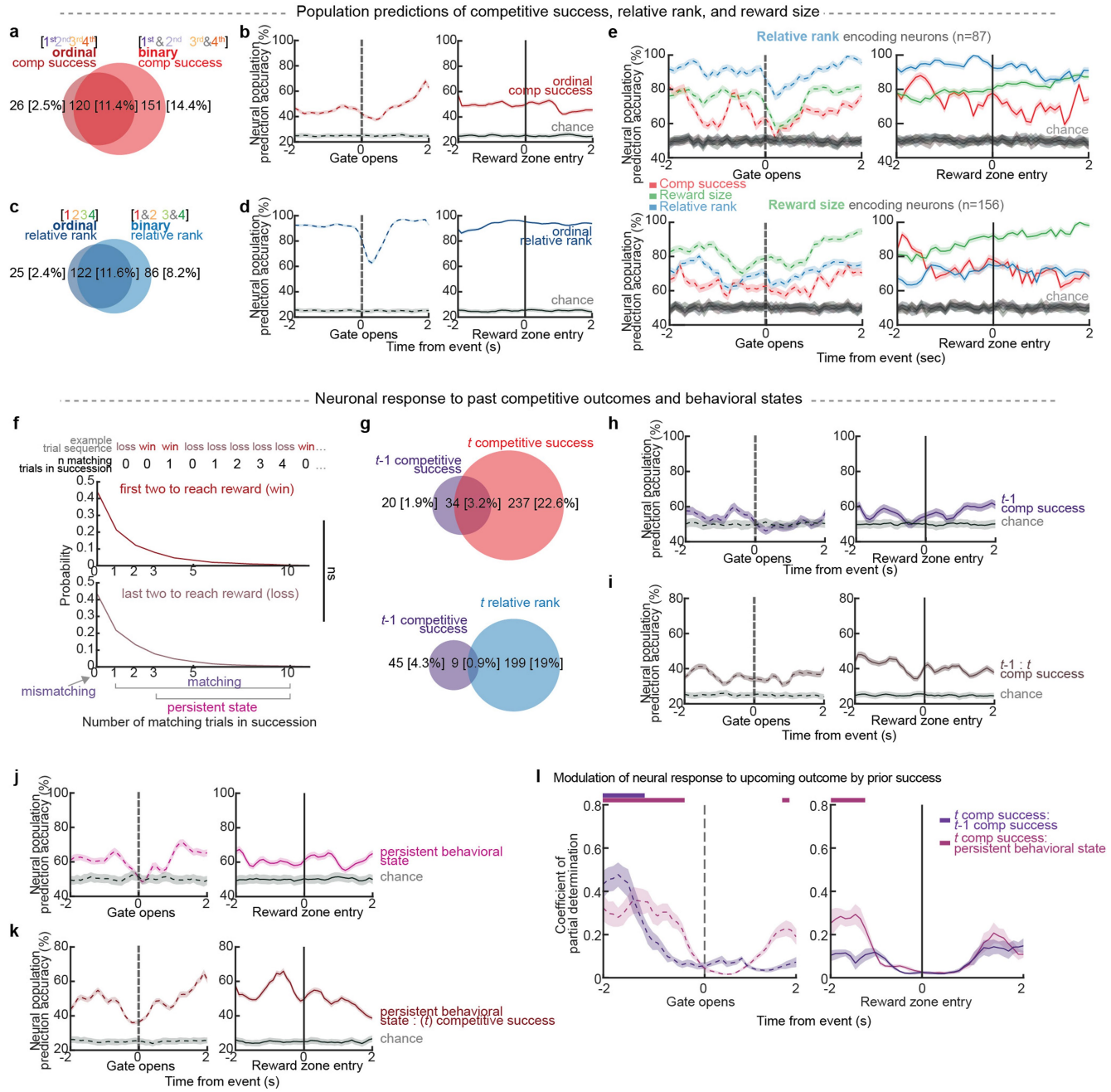nt 25th/75th percentiles with centre=median and whiskers=1st-99th percentile range. **i**, PETH and spike raster plots of two representative neurons that displayed changes in firing rate based on the animals' relative rank (high vs. low social rank in relation to the other animal). PETHs are aligned to the time point at which the recorded animal initiated an investigation of the other animal. Purple dots represent the end of an investigation. Shaded area denotes s.e.m. **j**, Top, Representative neuron during wireless recordings of the group foraging task (10 min after start of a session) compared to that of the two-chamber assay (3 h after start). Shaded area denotes s.e.m. Bottom, Venn diagram depicting the number of neurons encoding relative rank ($p<0.01$; Wilcoxon signed-rank) during the two-chamber assay and their overlap with those encoding relative rank during the group foraging task (n=115 overlap; $\chi^2_{(1)}=42.17$, $p=8.35\times10^{-11}$; Chi-Square test). **k**, Correlation of normalized firing rates for neurons that encoded relative rank during the group foraging vs. two-chamber assay on a cell-by-cell basis (n=115 RR-encoding of n=174 total rank-encoding neurons; r=0.673, $p=2.85\times10^{-24}$; Pearson correlation). Grey line depicts linear line of best fit. **l**, Decoding accuracy of relative rank during the two-chamber assay (n=942) was significantly higher than chance ($p=0.0024$, Permutation test) but lower than the peak decoding accuracy during the group foraging task (*$p=0.013$, Permutation test). **m**, SVM models trained on neuronal activity recorded during group foraging was used to decode validation data recorded during the two-chamber setup (i.e., switch model) or vice versa. Decoding accuracy for both switch models were significantly higher than expected from chance ($p=0.0031$ for group foraging model used to decode two-chamber data, $p=0.021$ for two-chamber model used to decode group foraging data; Permutation test). Overall, the group foraging model was better at decoding two-chamber rank rather than vice versa ($p=0.026$, Permutation test). Error bars denote mean±95%CI. N=500 bootstrapped samples for all decoding results.

Article
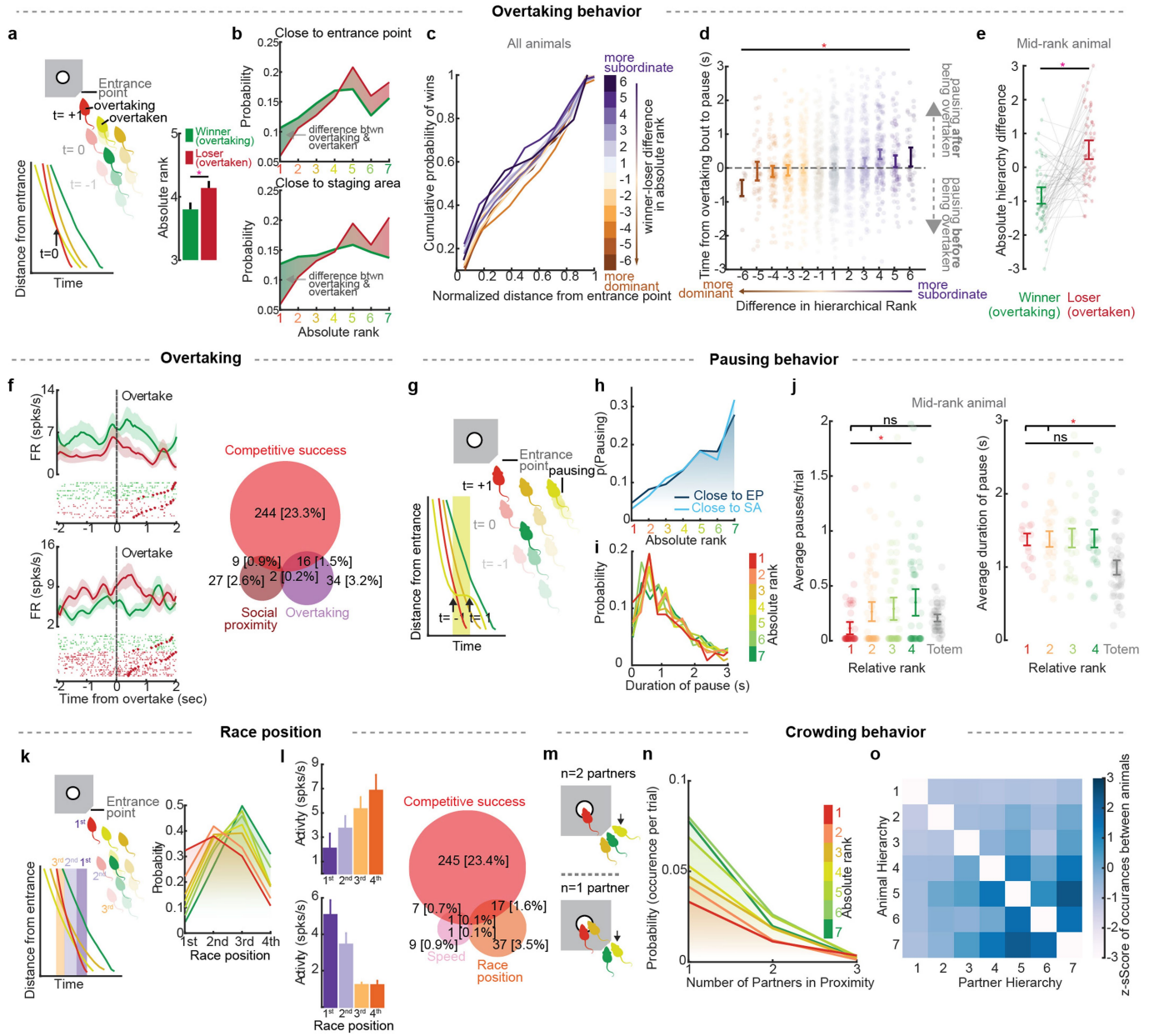
Extended Data Fig. 7 | See next page for caption.

Extended Data Fig. 7 | Neuronal responses to physical interaction between animals during competitive bouts. a, Graphic depicting an overtaking event where an animal (red, overtaking) overtakes another (yellow, overtaken) in the middle of running the trial. Right, overtaking animals were more likely to be higher ranking than the overtaken animals (n=4105 total overtaking events; *Z=-3.95, p=7.75x10-5; Signed-rank). **b**, Plot demonstrating the likelihood of being the overtaking animal based on absolute rank and position within the arena (n=4105 total overtaking events; Top, close to entrance point; Bottom, close to the staging area). **c**, Cumulative distribution function (CDF) demonstrating that overtaking events for higher ranked animals were more likely to occur farther away from the entrance point (closer to the staging area). N=4105 total overtaking events. **d**, The animals being overtaken were more likely to pause after an overtaking even when they were lower in rank than their competitors (*r_s=0.14, p=1.21x10^{-10}; Spearman correlation). Dots represent one overtaking/pausing bout (n=2074 total). Based on GLMs that further took into account the animals' previous trial performance (Methods), there was a significant effect on the probability of a pausing event after an overtaking event based on rank difference (t_{3145}=-2.77, p=0.0088), velocity difference (t_{3145}=-11.02, p=2.99x10^{-28}) proximity between animals (t_{3145}=-5.68, p=1.32x10^{-8}), race position (t_{3145}=-6.53, p=2.99x10^{-13}) and distance from reward (t_{3145}=9.91, p=3.78x10^{-23}). **e**, The mid-ranked (recorded) animals were more likely to be ranked higher than another when overtaking them and more likely to be ranked lower when being overtaken (n=1221 overtaking events involving mid-ranked mouse; *Z=-4.08, p=4.43x10^{-5}; Signed-rank). **f**, Left, PETH and raster plots illustrating two representative cells that displayed a difference in their activities based on whether the recorded animal were overtaking another animal or being overtaken. Right, Most neurons that responded to differences in the animals' competitive success across groupings displayed little response to physical factors such as proximity to the other animals ($\chi^2_{(1)}$=232.3, p=1.88x10^{-52}; Chi-Square test) or overtaking events at which time the recorded animals

overtook another animal in their group ($\chi^2_{(1)}$=214, p=1.82x10^{-48}; Chi-Square test). **g**, Graphic depicting pausing behaviour, where an animal (yellow) pauses in the middle of running a trial. **h**, Lower ranked animals were more likely to pause while foraging with higher ranked animals no matter the spatial location. **i**, There was no difference in pause durations based on absolute rank ($\chi^2_{(6,7129)}$=2.04, p=0.067; Kruskal-Wallis). **j**, Left, mid-rank (recorded) animals paused more often when they were lower in rank than their competitors (*r_s=0.17, p=0.007) but displayed no difference in pausing behaviour when running with totems compared to group trials (Z=-2.28 p=0.26; Signed-rank). Right, The total duration of pauses by the mid-ranked animals were not influence by relative rank (r_s=-0.02, p=0.85) but was significantly shorter when running with totem trials compared to group trials (Z=-4.76 p=1.9x10^{-6}; Signed-rank). Dots represent session averages (n=63). **k**, Graphic depicting physical race positions based on the animals' closeness to the reward zone in relation to others on trials that had an overtaking event. Right, the dominant animals were more likely to be in a higher race position. **l**, Left, Bar plots of two representative neurons that were tuned to the animals' instantaneous position during a trial. Error bars denote mean ± s.e.m. Right, Most neurons that responded to differences in competitive success across groupings displayed little response to the animal's physical position in relation to others ($\chi^2_{(1)}$=205, p=1.66x10^{-46}; Chi-Square test). **m**, Graphic depicting events in which the animals are crowded outside the entrance point, where the target animal (yellow) is in proximity with either two (Top) or one (Bottom) other competitor. **n**, Animals that were lower in relative rank were more likely to crowd with one or two others compared to animals that were higher in relative rank. N=3819 total crowding events. **o**, Heat map demonstrating that, during crowding events, animals of lower relative rank were more commonly partnered with other animals of lower relative rank. Error bars and shaded areas denote mean±95%CI.

Population predictions of competitive success, relative rank, and reward size

Neuronal response to past competitive outcomes and behavioral states

Extended Data Fig. 8 | See next page for caption.

Extended Data Fig. 8 | Effect of past interactions, relative rank and reward on neuronal response. a, Venn diagram depicting the number of neurons encoding the animals' ordinal (i.e., first vs. second vs. third vs. fourth to reach reward entry zone) competitive success overlapping with neurons encoding binary (i.e., first two vs last two to reach reward entry zone) competitive success (p<0.01, FDR corrected for multiple epochs). Most neurons that encoded the animals' ordinal and binary competitive success overlapped (n=120; $\chi^2_{(1)}$=30.7, p=3x10^{-8}; Chi-Square test). **b**, Decoding accuracy for ordinal competitive success for all task-modulated neurons (n=560; p<0.05; Permutation tests). Decoding accuracy gradually increased to a peak of 63.2±1.5% prior to reward zone entry (p<0.001, Permutation test). **c**, Venn diagram depicting the degree of overlap between neurons encoding the animals' ordinal relative rank (i.e., first vs. second vs. third vs. fourth) and binary (i.e., two highest vs two lowest) relative rank (p<0.01, FDR corrected for multiple epochs). Neurons encoding the animals' ordinal relative rank almost entirely overlapped with those that encoded the animal's binary relative rank (n=122 overlap; $\chi^2_{(1)}$=29.3, p=6.24x10^{-8}; Chi-Square test). **d**, Using all task-modulated neurons (n=560), decoding accuracy for ordinal relative rank were significantly higher than chance over the course of the trials (p<0.0001; Permutation tests). **e**, Decoding accuracies for relative rank and reward size using only neurons that encoded relative rank (Left, n=87) or reward size (Right, n=156), respectively. **f**, Recent history effects. Top, example trial sequence and count of cumulative matching trials in succession. Bottom, number of 'matching' trials in succession when comparing wins vs losses at trial t (Z=1.013, p=0.31; Rank-sum) suggesting transient, short-lasting successions of wins and losses. N=4966 total trials. **g**, Venn diagrams depicting the number of neurons encoding competitive success in the past trial t-1 and their overlap with neurons encoding competitive success (Top) or relative rank (Bottom) in the present trial t (p<0.01, two-way ANOVA, FDR corrected for multiple epochs). Most neurons that encoded the animals past success (5.1%, n=54) overlapped with those that encoded their current success (n=34; $\chi^2_{(1)}$=1.31, p=0.25; Chi-Square test) but were largely distinct from those that encoded the animals' relative rank (n=9; $\chi^2_{(1)}$=12.2, p=0.00046; Chi-Square test). **h**, Using all task-modulated neurons (n=560), decoding accuracies for the previous trial competitive outcome (t-1) were not significantly different than chance (p>0.05; Permutation tests). Peak decoding accuracy for past success was 57.2±2.3% (H$_0$=50% chance performance; p>0.05; Permutation tests). **i**, Using all task-modulated neurons (n=560), decoding accuracies for the animal's current success (t) contingent on the previous trial's competitive outcome (t-1) was significantly higher than chance (p<0.01; Permutation tests). These neurons predict the animal's current success contingent on their past outcome with accuracy of up to 41.3±3.1% prior to trial onset (H$_0$=25%, p<0.001; Permutation test). **j**, Using all task-modulated neurons (n=560), considering succession of wins or losses (behavioural states), decoding accuracy for the animals' behavioural state prior to gate opening was 66.2±2.0% (H$_0$=50% chance performance; p<0.01, Permutation test). **k**, Using all task-modulated neurons (n=560), peak decoding accuracy for the animals upcoming success contingent on their prior behavioural state prior to gate opening was 64.7±3.7% (H$_0$=25% chance performance; p<0.001; Permutation test). **l**, GLMs were used to quantify the contribution of past behaviour to neural population response for competitive success (Methods). Time points in which the fraction of explained variance for the interaction between terms was higher than expected from chance (p<0.01; Permutation test). Trials are aligned to the gate opening or time point at which the recorded animal reached the reward zone. Shaded areas denote mean±95%CI. N=500 bootstrapped samples for all decoding results.
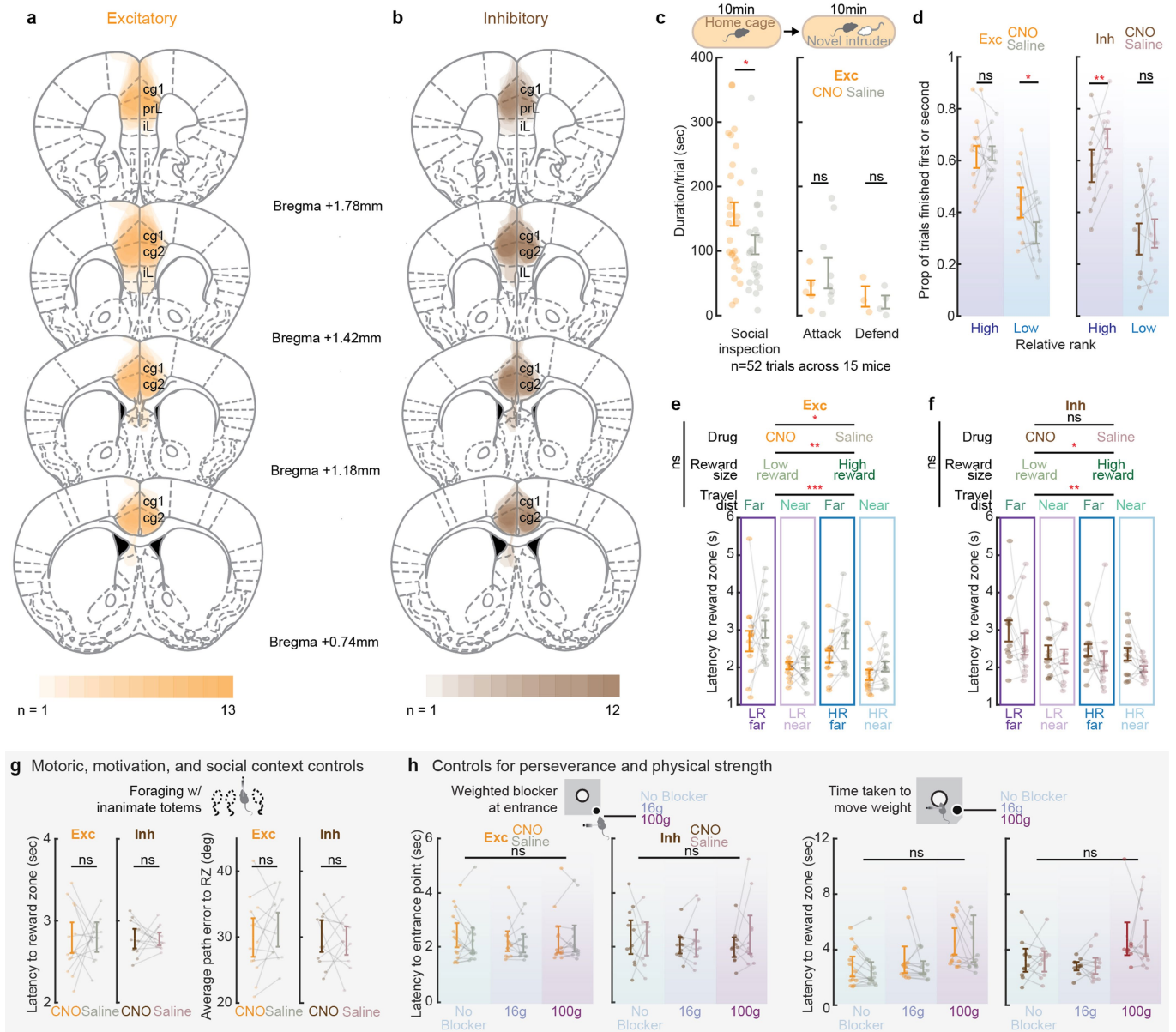
Extended Data Fig. 9 | DREADD manipulation of the ACC selectively influences competitive effort but not motivation or reward-seeking behaviour. a, **b**, Overlay of viral expression areas for **a**. hM3D(Gq)-mCherry across 13 animals and for **b**. hM4D(Gi)-mCherry across 12 animals. cg1/cg2=cingulate areas 1/2; prL=prelimbic cortex; iL=infralimbic cortex. **c**, Novel intruder assay for social aggression. Although the animals displayed an increase in social inspection behaviours following CNO compared saline (Left, *Z=1.77, p=0.038, one-sided rank sum), they displayed no change in attack or defensive behaviours (Right, p>0.3, two-sided Rank-sum). N=52 trials across n=15 animals. **d**, The likelihood of competitive success was higher for ACC excitation (Left, n=13, compared to saline) in trials where they were of lower relative rank (relative rank 3 or 4) than their competitors (*$t_{(12)}$=2.63, p=0.011; Paired t-test), but not when they were higher in relative rank (relative rank 1 or 2) than their competitors ($t_{(12)}$=-0.24, p=0.59; Paired t-test). Right, The likelihood of competitive success was decreased for ACC inhibition (n=12, compared to saline) in trials where they were of higher relative rank (relative rank 1 or 2) than their competitors (**$t_{(11)}$=-2.11, p=0.028; Paired t-test), but not when they were of lower relative rank (relative rank 3 or 4) than their competitors ($t_{(11)}$=-0.25, p=0.4; Paired t-test; Fig. 4e). **e**, Animals with ACC excitation reached the reward zone faster (n=13, *$F_{(1,109)}$=3.98, p=0.049) in high compared to low reward trials (**$F_{(1,109)}$=4.33, p=0.04) and when starting in the near compared to far staging areas (***$F_{(1,109)}$=27, p=1.04x10^{-17}), but there were no interactions between any of

the conditions ($F_{drug:reward(1,109)}$=0.23, p=0.63; $F_{drug:stagingarea(1,109)}$=0.66, p=0.42; $F_{reward:stagingarea(1,109)}$=0.52, p=0.47; three-way ANOVA). **f**, Animals with ACC inhibition reached the reward zone faster in high compared to low reward trials (n=12, *$F_{(1,95)}$=5.1, p=0.026) and when starting in the near compared to far staging areas (**$F_{(1,95)}$=4.1, p=0.046), but there were no interactions between any of the conditions ($F_{drug:reward(1,95)}$=0.13, p=0.72; $F_{drug:stagingarea(1,95)}$=0.043, p=0.84; $F_{reward:stagingarea(1,95)}$=0.51, p=0.33; three-way ANOVA). **g**, Mice foraging alone with inanimate totems. Left, There was no difference in latency to reach reward for either ACC excitation (n=13 mice, $t_{(12)}$=-0.058, p=0.96; Paired t-test) or inhibition (n=12 mice, $t_{(11)}$=0.051, p=0.96; Paired t-test). Right, There was no difference in average path error to reaching the reward zone for either ACC excitation ($t_{(12)}$=-0.79, p=0.44; Paired t-test) or inhibition ($t_{(11)}$=0.47, p=0.65; Paired t-test). **h**, Mice moving a mass of variable weight to receive reward. Left, there was no difference in the latency to reach the reward zone based on differences in weight (low vs. high) for either ACC excitation (n=14 sessions across n=13 mice, $F_{(2,77)}$=0.07, p=0.93; Two-way ANOVA) or inhibition (n=12 sessions across n=12 mice, $F_{(2,67)}$=0.58, p=0.56; Two-way ANOVA). Right, There was no difference in the latency to push past the weight to reach the reward zone for either ACC excitation ($F_{(2,77)}$=0.85, p=0.8; Two-way ANOVA) or inhibition ($F_{(2,67)}$=0.01, p=0.99; Two-way ANOVA). Error bars denote mean ± s.e.m. Dots represent session averages. N=6 mice for Exc group and n=6 mice for Inh group.
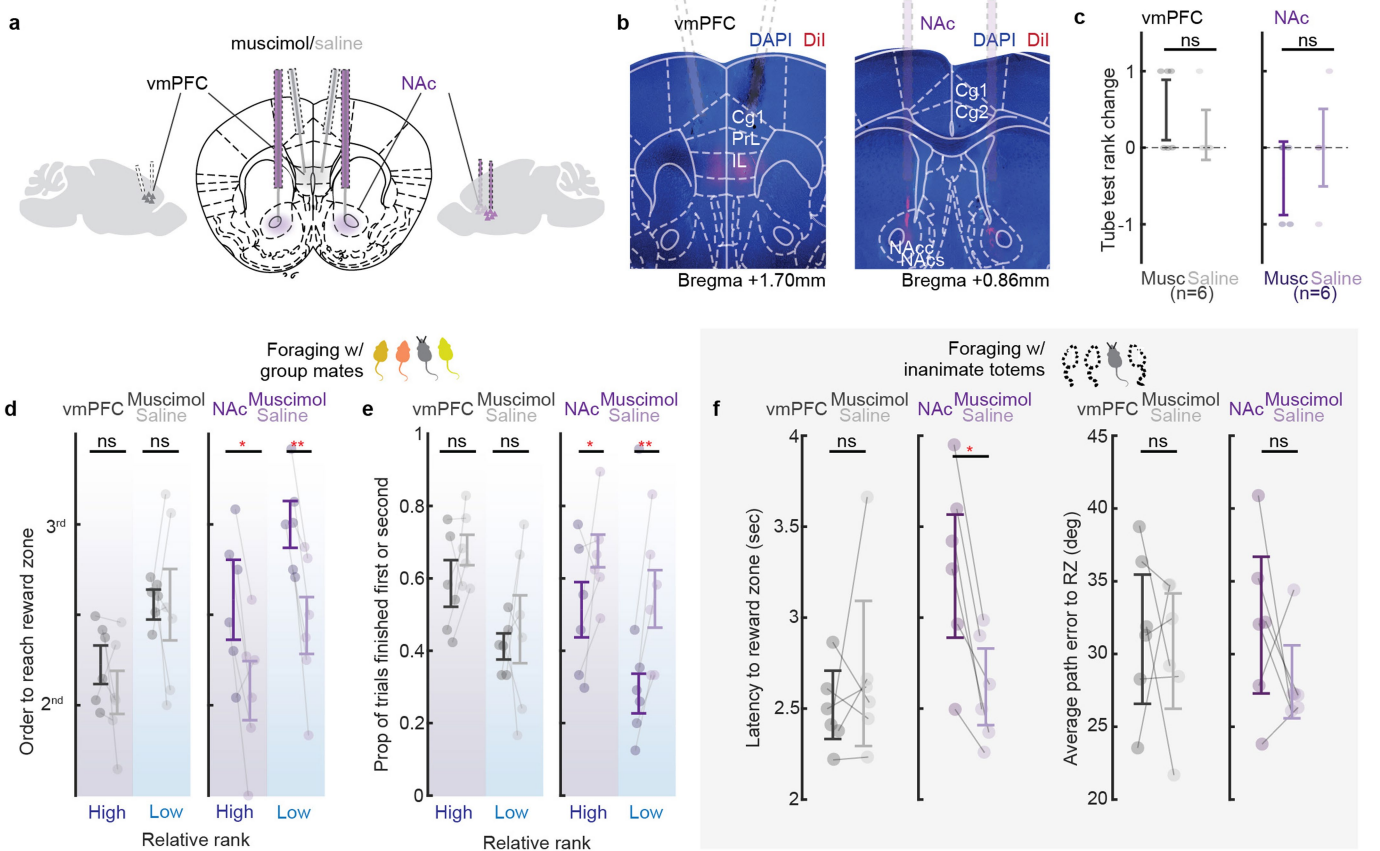
Extended Data Fig. 10 | Nonselective effects of vmPFC and NAc inhibition on competitive behaviour. a, Schematic illustrating reversable musicmol inactivation in either the ventromedial prefrontal cortex (vmPFC) or the nucleus accumbens (NAc; Methods). **b**, Representative histological images displaying the muscimol injection sites for the vmPFC (Left) and NAc (Right). **c**, Animals injected with muscimol did not display a change in absolute social rank in the tube test compared to saline for either the vmPFC (Left, n=6 mice, Z=1, p=0.32, Signed-rank) or the NAc (Right, n=6 mice, Z=-1, p=0.32, Signed-rank). Error bars denote mean±95%CI. **d**, Group competition. Left, animals injected with muscimol in the vmPFC did not display a difference in the competitive order to reaching reward when compared to saline (p>0.2; Paired t-tests). Right, animals injected with muscimol in the NAc displayed a decrease in the competitive order to reaching reward when compared to saline, but this effect was observed both when the animals' relative rank was either higher (*$t_{(5)}$=2.51, p=0.027; Paired t-test) or lower (**$t_{(5)}$=3.12, p=0.013; Paired t-test) than their competitors. Error bars denote mean ± s.e.m. **e**, Group competition. Left, animals injected with muscimol in the vmPFC did not display a difference

in reaching reward first or last when compared to saline (>0.05; Paired t-tests). Right, animals injected with muscimol in the NAc displayed a decrease in likelihood of reaching reward first when compared to saline, but this effect was observed both when the animals' relative rank was either higher $t_{(5)}$=-2.17, p=0.041; Paired t-test) or lower (**$t_{(5)}$=-2.8, p=0.019; Paired t-test) than their competitors. Error bars denote mean ± s.e.m. **f**, Foraging with totems. Left, animals injected with muscimol in the vmPFC did not display a difference in latency to reaching the reward zone ($t_{(5)}$=-0.85, p=0.42; Paired t-test). Animals injected with muscimol in the NAc displayed an increase in latency (*$t_{(5)}$=0.2.08, p=0.046; Paired t-test). Right, animals injected with muscimol in the vmPFC did not display a difference in the average path error to the reward zone ($t_{(5)}$=0.17, p=0.87; Paired t-test). Animals injected with muscimol in the NAc also did not display a difference in the average path error to the reward zone NAc ($t_{(5)}$=0.44, p=0.34; Paired t-test) together suggesting that NAc inactivation decreased the animals' effort across both social and non-social conditions without affecting their overall motoric ability[20]. Error bars denote mean ± s.e.m. For panels **c–f**, n=6 mice for vmPFC group and n=6 mice for NAc group.

nature portfolio

Corresponding author(s):	Ziv Williams
Last updated by author(s):	Jul 7, 2021

Reporting Summary

Nature Portfolio wishes to improve the reproducibility of the work that we publish. This form provides structure for consistency and transparency in reporting. For further information on Nature Portfolio policies, see our Editorial Policies and the Editorial Policy Checklist.

Statistics

For all statistical analyses, confirm that the following items are present in the figure legend, table legend, main text, or Methods section.

n/a	Confirmed	
☐	☒	The exact sample size (n) for each experimental group/condition, given as a discrete number and unit of measurement
☐	☒	A statement on whether measurements were taken from distinct samples or whether the same sample was measured repeatedly
☐	☒	The statistical test(s) used AND whether they are one- or two-sided *Only common tests should be described solely by name; describe more complex techniques in the Methods section.*
☐	☒	A description of all covariates tested
☐	☒	A description of any assumptions or corrections, such as tests of normality and adjustment for multiple comparisons
☐	☒	A full description of the statistical parameters including central tendency (e.g. means) or other basic estimates (e.g. regression coefficient) AND variation (e.g. standard deviation) or associated estimates of uncertainty (e.g. confidence intervals)
☐	☒	For null hypothesis testing, the test statistic (e.g. F, t, r) with confidence intervals, effect sizes, degrees of freedom and P value noted *Give P values as exact values whenever suitable.*
☒	☐	For Bayesian analysis, information on the choice of priors and Markov chain Monte Carlo settings
☒	☐	For hierarchical and complex designs, identification of the appropriate level for tests and full reporting of outcomes
☐	☒	Estimates of effect sizes (e.g. Cohen's d, Pearson's r), indicating how they were calculated

Our web collection on statistics for biologists contains articles on many of the points above.

Software and code

Policy information about availability of computer code

Data collection	Ethovision XT12 and XT13 for 2-d behavioral tracking and collection; TBSI W16 system paired with a Plexon MAP data acquisition system for neuronal processing and collection; Keyence BZ-X800 for immunofluorescence
Data analysis	All data processing and analyses were performed in MATLAB 2019b (and above); ImageJ version 1.52 for histological images. The behavioral and neuronal data that support the findings of this study are available from the corresponding author upon reasonable request. All software used in this study are listed in the Reporting Summary along with their versions. The custom MALAB codes used to perform data and statistical analyses that support the findings of this study are available from the corresponding author upon reasonable request.

For manuscripts utilizing custom algorithms or software that are central to the research but not yet described in published literature, software must be made available to editors and reviewers. We strongly encourage code deposition in a community repository (e.g. GitHub). See the Nature Portfolio guidelines for submitting code & software for further information.

Data

Policy information about availability of data

All manuscripts must include a data availability statement. This statement should provide the following information, where applicable:
- Accession codes, unique identifiers, or web links for publicly available datasets
- A description of any restrictions on data availability
- For clinical datasets or third party data, please ensure that the statement adheres to our policy

The data and primary codes that support the findings of this study data are available from the corresponding author upon reasonable request.

Field-specific reporting

Please select the one below that is the best fit for your research. If you are not sure, read the appropriate sections before making your selection.

☒ Life sciences ☐ Behavioural & social sciences ☐ Ecological, evolutionary & environmental sciences

For a reference copy of the document with all sections, see nature.com/documents/nr-reporting-summary-flat.pdf

Life sciences study design

All studies must disclose on these points even when the disclosure is negative.

Sample size	No statistical method was used to determine the sample size for animal experiments. The number of animals for both the neurophysiological recording (n=7) and manipulation (n=25 for DREADD and n=6 for muscimol) experiments meet standards in the field. Number of unique groups (n=14, for a total of 98 male mice) was determined by the sample sizes used in previous studies investigating dominance hierarchies in rodents (Wang et al., 2011; Kingsbury et al., 2019; Zhoue et al., 2017). Specific sample sizes are described in the manuscript.
Data exclusions	No sessions or trials were excluded from any behavioral analyses. The first trial of each experimental block was excluded from analyses to avoid condition-switching effects. One mouse from the excitatory DREADD groups and 2 mice from the inhibitory DREADD groups were excluded due to null viral expression. For the dynamic non-social context control, Two sessions were excluded where animals were consistently accidentally tripped by the fishing line. For electrophysiological recordings, unstable single units that either appeared, dropped out or shifted (in principal component space) were excluded.
Replication	All behavioral experiments were performed with multiple groups with animals from several litters, across many sessions. Each cohort displayed similar behaviors and no sessions were excluded from the main experiments. For the dynamic non-social control, two sessions were excluded where animals were consistently accidentally tripped by the fishing line. For neuronal recordings, all 7 animals displayed similar population properties. All experiments were replicated over a 1.5 year period and were all performed independently. All attempts at replications were successful. Groups of mice not displaying stable transitive dominance hierarchies across 3 consecutive weeks were excluded prior to experimentation.
Randomization	For all experiments, age- and weight-matched naïve mice were randomly allocated in groups of seven animals to prevent potential behavioral confounds arising from kin. Animals were randomly assigned to one of seven color dyes for behavioral tracking, and to groups for all viral injections and cannulae placements. Sequence during behavioral experiments were pseudo-randomized (see 'Methods').
Blinding	Experimenters were blinded to the hierarchical rank of animals for all behavioral experiments and analyses requiring manual scoring (e.g. social interactive behaviors during resident intruder assay, and urine marking assay). Blinding was not possible for DREADD experiments where CNO or saline was injected since the solutions were mixed prior to injections, and not possible for cannulae experiments where muscimol or saline was injected. For all other experiments (including electrophysiological recordings and behavioral control experiments), experimenters were blinded to group allocation or experimental condition (e.g. weight of blocker) during data collection. In all experiments, experimenters were blinded to all experimental conditions during data analyses.

Reporting for specific materials, systems and methods

We require information from authors about some types of materials, experimental systems and methods used in many studies. Here, indicate whether each material, system or method listed is relevant to your study. If you are not sure if a list item applies to your research, read the appropriate section before selecting a response.

Materials & experimental systems

n/a	Involved in the study
☒ ☐	Antibodies
☒ ☐	Eukaryotic cell lines
☒ ☐	Palaeontology and archaeology
☐ ☒	Animals and other organisms
☒ ☐	Human research participants
☒ ☐	Clinical data
☒ ☐	Dual use research of concern

Methods

n/a	Involved in the study
☒ ☐	ChIP-seq
☒ ☐	Flow cytometry
☒ ☐	MRI-based neuroimaging

Animals and other organisms

Policy information about studies involving animals; ARRIVE guidelines recommended for reporting animal research

Laboratory animals	C57BL/6J male mice, aged 2 to 5 months, were maintained on a 12-hour light/dark cycle (6am to 6pm) at 70degF at 40-60% humidity, and were provided food and water ad libitum outside of behavioral testing periods for foraging tasks. For all foraging tasks, animals were kept at 85% of baseline body weight and had free access to water. All experiments were performed in the light phase of the 12-hour cycle.

Wild animals	No wild animals were used in the study
Field-collected samples	No field collected samples were used in the study
Ethics oversight	NIH Guidelines for the Care and Use of Laboratory Animals; Massachusetts General Hospital IACUC

Note that full information on the approval of the study protocol must also be provided in the manuscript.